QUEENSLAND INSTITUTE OF TECHNOLOGY

DEPARTMENT OF PHYSICS

MEASUREMENT OF RADON DAUGHTERS

D. Bromwich

December 1980

QUEENSLAND INSTITUTE OF TECHNOLOGY

DEPARTMENT OF PHYSICS

MEASUREMENT OF RADON DAUGHTERS

D. Bromwich

December 1980

ABSTRACT

The application of β - α delayed coincidence to the measurement of 214 bismuth/214 polonium has been investigated. A technique using simple electronic circuits and detectors is demonstrated, and shows promise as a low cost 'working level' meter for uranium mining. The device would be isotope specific for 214 polonium and have high background rejection for environmental monitoring.

ACKNOWLEDGEMENTS

I wish to thank my supervisors Dr. B. J. Thomas and Mr. B. M. O'Leary of the Department of Physics, Queensland Institute of Technology, for their invaluable advice and guidance.

I would also like to thank the Department of Physics technical staff for their able assistance in constructing items for this project and for repairing equipment, especially Mr. M. K. Power, Mr. J. A. Jull, Mr. B. Wheeler and Mr. R. Galloway.

I am grateful to Dr. D. E. Allen of the Department of Medical Technology, Queensland Institute of Technology for offering the use of his electron microscope facility, Mr. I. Coombe for performing electron microscopy and Ms. G. Green for preparing the prints.

I am also indebted to Mr. M. Ilic of the Department of Mathematics, Queensland Institute of Technology, for bringing to my attention alternate approaches to geometric factors.

I would also like to thank Watson-Will and Company for providing a sample of mylar film.

Finally, I wish to thank my wife, Christine, for her tolerance and assistance, especially during the final stages of the project.

TABLE OF CONTENTS

		PAGE		
	ABSTRACT			
	ACKNOWLEDGEMENTS			
1	INTRODUCTION			
	1.1 Scope of Report	2		
	1.2 Delayed Coincidence	2		
	1.3 Health Hazards	4		
	1.4 Working Level	5		
2	METHODS OF SAMPLING AND ANALYSIS OF RADON DAUGHTERS	7		
	2.1 Introduction	7		
	2.2 Filter Methods	7		
	2.3 Scintillation Methods	8		
	2.4 Integrating Methods	9		
3	PRELIMINARY INVESTIGATIONS	10		
	3.1 Delayed Coincidence System	10		
	3.2 Feasibility Study	13		
4	EXPERIMENTAL PROCEDURE	18		
	4.1 Oil Experiment	18		
	4.2 Two Filter Tube	18		
	4.3 Radon Generator	18		
	4.4 The "System"	19		
	4.5 Theory of Operation of "System"	20		
	4.6 γ Ray Spectroscopy	20		
	4.7 Experimental Procedure	21		
5	RESULTS	23		
•	5.1 Multichannel Scaling (MCS)	23		
	5.2 "System" Gate Optimization	27		
	5.3 Channel Dead Time	28		
	5.4 Flow Meter Calibration	30		
	5.5 Results of System Performance	31		
	5.5.1 Initial Daughter Equilibrium	32		
	5.5.2 Run 1 Data	34		
	5.5.3 Run 2 Data	37		
	5 5 4 Run 3 Data	38		

				PAGE
	5.6	Analys	is of Data	41
		5.6.1	Dynamic Response	41
		5.6.2	RaB Evaluation	42
		5.6.3	RaA Assessment	43
		5.6.4	Coincidence Count Repeatability	43
		5.6.5	Calibration	44
			Lower Level of Detection	46
		5.6.7	Measurement of Individual Daughters to Determine WL	47
6	DISC	USSION		52
	6.1	Summar	y of Results	52
	6.2	Compar	ison of Other Methods	53
	6.3	Improv	ements	54
7	CONC	LUSION		55
	REFE	RENCES		56
	APPE	NDIX 1	Geometric Factor	63
	APPE	NDIX 2	Rapid Decay Correction	67
	APPE	NDIX 3	Properties of Radon	68
	APPE	NDIX 4	Two Filter Tube and Planchet	71
	APPE	NDIX 5	Model of System	74
	APPE	NDIX 6	Recoil Losses	79
	APPE	NDIX 7	Electron Microscopy	82
	APPE	NDIX 8	Oil Experiment	84
		NDIX 9	1	86
-			Multiscaling Half-Life Error	89
	APPE	NDIX 11	Geiger Muller Tubes	90
	APPF	NDTX 12	Dead Time and Error	91

INTRODUCTION

In the dosimetry of radon and its daughters, it is important to determine not only the gross activity but also the proportion of the activity due to the individual daughters - i.e. the state of equilibrium. Counting techniques of various levels of sophistication have been developed for these purposes. This report considers an investigation of a technique new to this area.

A survey of the literature [HOLADAY 1956, BUDNITZ 1974, CLIFF 1978, PERDUE 1980] showed that the common techniques for measuring the concentrations of the short lived daughters of radium did not exploit the very short half life of 164µs for RaC' (214Po). The decay scheme below for the 238 uranium series shows this half life to be many orders of magnitude lower than that of the other short lived daughters - RaA, RaB, RaC.

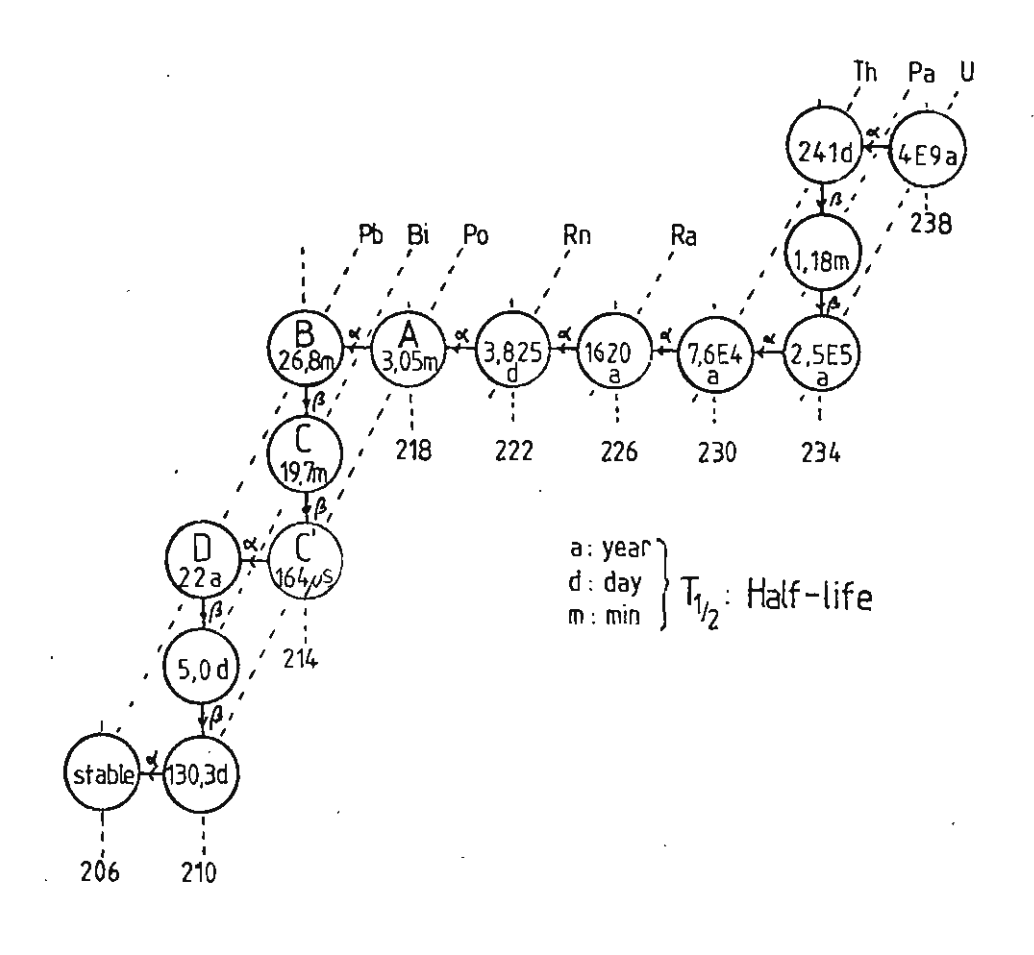


FIGURE 1 DECAY SCHEME FOR 238 URANIUM

Detection of two near coincident decays would be specific for RaC/RaC' and virtually free from background interference.

RaC may even be considered as a double decay with RaC' as an intermediate metastable state.

Random coincidence associated with high count rates would be expected to be negligible as environmental air activities of samples containing these short lived daughters produced by the decay of 222-radon gas would be unlikely to give rise to count rates of hundreds of counts per second in any detector.

1.1 Scope of Report

This report investigates the application of these near coincidence decays to measure radon daughters with a method called "delayed coincidence". The investigation covers a feasibility study and the development of a prototype instrument. A short analysis of some of the results follows. The Appendices cover some of the mathematical aspects of the study, working drawings of apparatus and detail not directly related to the study.

1.2 Delayed Coincidence

A deeper search of the literature towards the end of the study revealed the concept of delayed coincidence had been used previously in different forms in environmental monitoring. The closest to the present technique is that of RANKIN (1963) who used β - α delayed coincidence to reduce the effect of radon and thoron background on an air filter to allow the determination of 239 plutonium. Though unimportant to the technique, the analysis appears confused since radon does not collect on filters, although the more chemically active daughters do. (This is the principle of the "two filter method" for radon (THOMAS, 1970)).

The activity on the filter would be almost entirely due to daughter activity which may or may not be in radioactive equilibrium. An immediate estimate of 239 plutonium activity may be made by applying a correction factor calculated from the incidence of detection of RaC β decay followed just before a RaC' α decay as shown in the figure below. The α background is reduced and the estimation may be made without having to wait for the radon and daughter background to decay.

α - β COINCIDENCE COUNTING OF RaC'

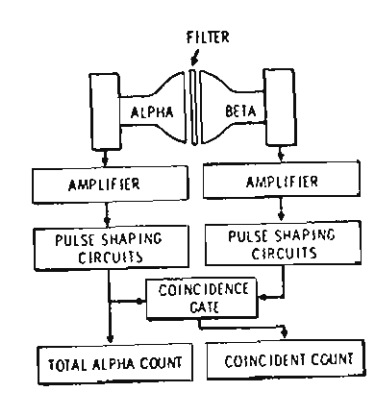


FIGURE 2 after RANKIN (1963)

The half life of RaC' has been demonstrated by ERLICK (1971) using a number of methods based on delayed coincidence. A similar technique was used in the feasibility study in this report and in a test of the prototype instrument.

A "fast pairs" technique using α - α delayed coincidence was used by GIFFEN (1963) to determine actinon (219 radon, T^1_2 3.92s) and thoron (220 radon, T^1_2 54.5s) concentrations in a scintillation chamber. The technique is limited to *very* low levels of mixed isotopes to ensure that mainly true delayed coincidence decays, not spurious decays are detected.

The α - α "fast pairs" technique has been briefly reviewed by CHERRY (1964) as an alternative to α -spectroscopy and recommends its use in analysing environmental samples for the short lived

 α -emitters 216 Polonium (T $\frac{1}{2}$ 0.158s) and 215 Polonium (T $\frac{1}{2}$ 0.0018s).

True coincidence methods have been used to determine radon daughter levels by $\beta-\gamma$ coincidence. Simultaneous detection of a β particle in a plastic scintillator and surrounding γ detectors has been used by BRAUER (1968) to detect "226 radium and daughters". A decrease in sensitivity but a large reduction in background is reported.

A review by KIEFER (1972) of delayed coincidence techniques for RaC and 216 polonium states "the method is of limited practical use because of the frequency of random coincidences". A model is developed in this study and tested to show that at expected environmental levels this is not a problem. Though the concept of delayed coincidence has been applied before, it seems that it has not been applied to the determination of radon daughters in a Working Level monitor.

1.3 Health Hazards

The need to measure radon and daughters is most important in the mining and processing of uranium ore (FRY 1975), though other types of mines (HOLADAY 1969, DUGGAN 1970, BOYD 1970) can produce high levels of radon and thoron.

The main area of interest is the radiobiological effect on the lung resulting from inhalation of radioactive material suspended in the air. This may be in the form of radioactive atoms or ions and may also be attached to various aerosol particles present. The physical properties, especially diffusivity and size of the attached and unattached fractions are very different (GEORGE 1972), but were not measured in this study.

The lung may be considered like a bellows - with air moving in and out with respiration. The function of the lung of primary importance is its filtering action (COMROE 1966). Particles larger than 10μ ($10^{-5}m$) are filtered by the nose, but particles down to

 2μ are trapped on the walls of the trachea, bronchi and bronchioles. Only particles between 2μ and 0.3μ are likely to reach the alveloli. Aerosols of smaller particles tend to stay suspended, but if deposited, may enter the bloodstream.

Against this tendency to deposit in the lungs is the co-ordinated wave action of the cilia lining the bronchioles to the nose, which transport a protective mucus sheet to the pharynx, carrying with it any deposited dust. The combination of this, the size distribution of the aerosol activity, the thickness of the mucus, the varying sensitivity of the basilar layers of the bronchotrachael epithelium, the rate of movement of the sheath of mucus and variations in the pulmonary geometry in individuals all contribute to a wide range in radiosensitivity to a given concentration of daughters. For control of the short-lived radium daughters (more commonly called radon daughters) a quantitative measure of the combined effect is needed. The "Working Level" is such a measure.

1.4 Working Level

The necessity to quantitate the potential radiobiological harm from inhalation of mine aerosols was developed to enable control of radon (and thoron) daughters. The Working Level (WL) is defined as any combination of the short lived daughters in one litre of air that will result in the ultimate emission of 1.3 x 10 MeV of potential alpha energy. To apply this to miners, the concept of the Working Level Month (WLM) is applied. The WLM is an exposure for 170 hours to 1-WL concentration. In Australia, the Australian Government has published a "code of practice" for the application of this concept. The code stipulates a maximum exposure of 4-WLM per year as well as other rules to limit exposure (AUST. GOVT. PUB. SERV. 1977).

To understand the reasoning behind the concept of the WL the following table will help.

Nuclide	α Energy MeV	Half-Life	Atoms in 3.7Bq (100pCi)	Ultimate α Energy/Atom M.eV	Total Ultimate α Energy MeVx10 ⁵ / 3.7Bq)
218 _{Po, RaA}	6.00	3.05m	977	6.00(RaA) +7.6%(RaC')	0.134 (10%)
214 _{Pb, RaB}	0.00	26.8m	8580	7.69(RaC¹)	0.660 (53%)
²¹⁴ Bi, RaC	0.00	19.7m	6310	7.69(RaC')	0.485 (38%)
214 _{Po, RaC'}	7.69	164µs	0.0009	7.69(RaC')	0.0
•	·	·		TOTAL	1 270 × 105 M × V

TOTAL

1.279x10⁵MeV

Round up to

 $1.3 \times 10^{5} MeV$

TABLE 1 COMPOSITION OF 1 WL FROM AN EQUILIBRIUM MIX OF RADON DAUGHTERS

It is interesting to note that the contribution of RaB to 1WL from equilibrium mix is 53%, eventhough RaB is not an α emitter. It is the 7.69 MeV α from RaC' which contributes most of the dose, so a very good estimate of the number of WL's present could be made by just determining the integral RaC' activity, with no assumptions as to the degree of equilibrium. The 'older' the air is, the better the approximation.

The same concept of the WL is applied to thoron daughters (220 radon).

A review of the shortcomings of the WL has been made by CROSS (1979).

2. METHODS OF SAMPLING AND ANALYSIS OF RADON DAUGHTERS

2.1 Introduction

The measurement of radon daughters requires a sampling process and a measurement process, but the two may be inseparable. The techniques currently used are all based on a small number of methods, generally determined by the sampling process. These may be loosely grouped as filter, scintillation and integrating methods. Each will be discussed briefly before the new technique, based on filter collection, is discussed.

2.2 Filter Methods

A rapid aspiration of respirable air through a membrane or glass filter effectively removes all of the radon daughter activity (PALTRIDGE 1967, HOLMGREN 1977), although appreciable "burial losses" - from α radiation being stopped within the filter when activity is captured beneath the filter surface, may occur with some types of filter. The advantage of a filter collection method is that rapid concentration of low levels of activity occurs, with a counting geometry determined largely by the filter. A non-uniform deposition of this activity does not matter (see Appendix 1) if the detector placed over the filter is larger than the filter. Recoil losses may also occur are discussed in Appendix 6. If the gross activity of all the daughters is counted, then in the absence of any assumptions regarding the degree of radioactive equilibrium, three separate measurements need to be made (TSIVOGLOU, 1953) to determine the activity of each of the radon daughters RaA, RaB and RaC. The activity of RaC' is taken as that of its parent, RaC. If a degree of equilibrium can be assumed, then a single measurement gives an approximate error of 13% due to this assumption (KUSNETZ 1956, HARLEY 1969, GROËR 1972)

Another more elaborate approach is the use of silocon surface barrier detectors to perform alpha spectroscopy (MARTZ 1969, TREMBLAY 1979). This is the basis of one commercial instrument (HARSHAW "ENVIRONMENTAL WORKING LEVEL MONITOR").

The 222 radon concentration in the sample air may be determined by placing a second filter a distance behind the first filter (ROLLE 1969). The RaA formed by 222 radon decay in the volume between filters is collected on the second filter and its activity gives an indication of levels of 222 radon in the air.

The method is used as the basis for a number of atmospheric radon monitors (NEWSTEIN 1971, SCHERY 1980). The method is reviewed by THOMAS (1970).

2.3 Scintillation Methods

The techniques using scintillation have generally applied more to the measurement of 222 radon than radon daughters. Such a technique is to coat a volume internally with zinc sulphide and observe the scintillations with a photomultiplier when a sample of air containing radon and radon daughters has been left to decay for a few hours, to leave only 222 radon amd fresh radon daughters for counting (LUCAS 1957). Zinc sulphide scintillators have been used in continuous monitors for α activity in air. The problem of "plating out" of daughter activity on sensitive surfaces may be avoided with a protective air sheath. (AGOPSOWICZ 1979, RANDOLPH 1971) A variation of this method is the use of electrostatic collection of radon daughters followed by zinc sulphide α detection (ROBERTS 1966, DALU 1971, PERDUE 1980).

Liquid scintillation for alpha radiation is another technique which can be used. The problems associated with α -liquid scintillation (McDOWELL 1979) are energy resolution, quenching and high background. The method has been applied to environmental radon measurements (PRICHARD 1977) and radium measurements (DARRALL 1973).

A third scintillation technique, uses the detection of gamma rays from radon daughters by NaI (Tł) scintillators. A cryogenic method of sampling radon is discussed by PERDUE (1980) in conjunction with gamma ray spectroscopy. It may be possible to apply β - α delayed coincidence techniques to liquid scintillation to give a measure of RaC. However, time did not permit an investigation of this possibility.

2.4 Integrating Methods

These methods (TLD and Track etch) are applicable to personnel dosimetry, although some WL monitors also incorporate them. The detectors are light, cheap and of small size. However, the equipment required to analyse them is not; an automated TLD (thermoluminescent dosimetry) reader may cost \$60,000 upwards and relating the readings to 'Working Levels' is difficult. There are a number of papers (GUGGENHEIM 1978, Mc CURDY 1969, FRIEDLAND 1980, GAMMAGE 1976) related to the use of TLD and similar methods for radon and radon daughter measurement.

An excellent review on the application of track etch films to radon dosimetry is given by FRANK (1977).

By their nature, these integrating methods are more suitable for use in *passive* detectors requiring little or no additional electronics or attention except when they are 'read'.

3. PRELIMINARY INVESTIGATIONS

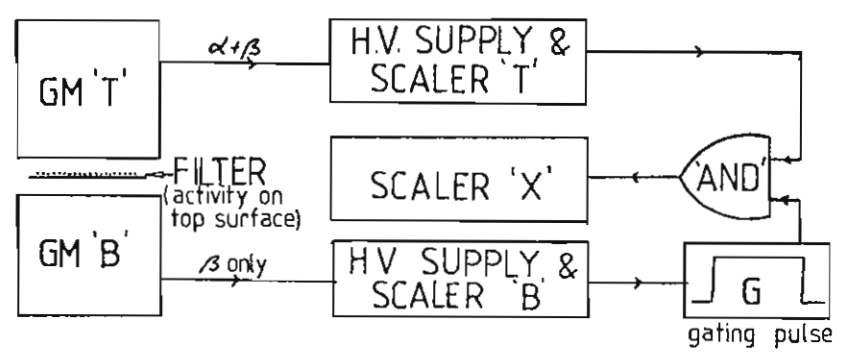
3.1 Delayed Coincidence System

This section discusses a feasibility study, and development and testing of a prototype system based on two Geiger Muller (GM) tubes (GEC model EHM2S).

The previous section referred to some different methods for measuring radon daughters - usually presented as simple, cheap and accurate. This may appear so in the laboratory, but may not stand up in field use. All the previous methods discussed have relied on (1) collection of a known volume of air and measuring its activity (Lucas flask) or by removing the activity from the sample volume (filter), or (2) by chance interaction of radiation with a passive detector, or (3) by electrostatic removal of the radioactive element from the air.

The technique developed here attempts to overcome some of the difficulties inherent in development of a practical instrument by relying on known reliable circuits for GM tubes and using membrane filters to collect the activity from the air. The new technique is based on two phenomena. First, the short half life of RaC' (214 polonium), which makes a β - α delayed coincidence detection of the RaC' α radiation isotope specific. Secondly, the range of environmental alpha particles is less than the thickness of the membrane filters used, for activity deposited on one surface. This enables the bottom GM 'B' to discriminate against α radiation.

The block diagram below shows the working of the system.



DELAYED COINCIDENCE BLOCK DIAGRAM
FIGURE 3

The filter has all its activity on, or very close to one surface, and is inserted active side up between the two GM detectors.

Membrane filtration of air containing radon and radon daughter activity results in complete collection of the radon daughters and no retention of any radon. With the parent radon removed a slight build-up activity still occurs on the filter after the radon daughters are deposited. Figure 4 below (after EVANS 1969) shows that the filter activity continues to increase for a short time following sampling, and only then decays. EVANS (1969) gives an excellent analysis of the process.

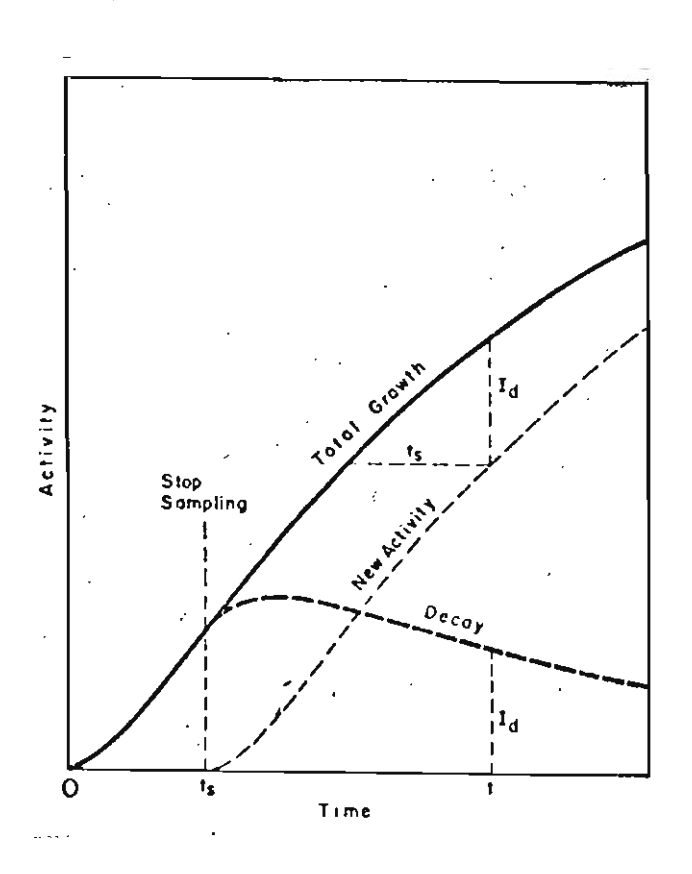


FIGURE 4 TOTAL DAUGHTER ACTIVITY ON FILTER
WITH TIME (after EVANS 1969)

The mathematical description of the decay of the series

RaA
$$\frac{\alpha}{3.05\text{m}}$$
 RaB $\frac{\beta}{26.8\text{m}}$ RaC $\frac{\beta}{19.7\text{m}}$ RaC' $\frac{\alpha}{164\mu\text{s}}$ RaD

is based on the decay constant $\lambda_{\hat{i}}$ of each component, and is described in terms of the "Bateman equations"

$$\frac{dNi}{dt} = N_{i-1} \lambda_{i-1} - N_i \lambda_i \text{ for } i - 1 \longrightarrow i$$

The slight increase in activity on the filter shown in Figure 4 post sampling is predicted by applying the equations and is mainly due to the antecedent activity of RaA.

Appendix 5 applies the mathematics describing the decay of the radon daughters to the "system performance".

The top GM 'T' in the system detects both α and β radiation from the decay series but the bottom GM 'B' can only detect β radiation, since the α activity is produced on the top surface of the filter and cannot pass, through it. This means only RaB and RaC are detected by 'B', not RaA and RaC'. For each count registered by the scaler attached to 'B', a pulse of length G (usually 400 μ S) is produced which opens the AND gate for any pulse from 'T' during that time. Since the half life of RaC' is only 164 μ s, the probability of an α particle being detected by 'T' during this sensitive period is high. A delayed coincidence event is registered on scaler X.

The coincidence scaler gives information related to RaC (and RaC'). The bottom scaler gives information relating to RaB and RaC. From this RaB concentrations may be deduced. The top scaler gives information regarding RaA, RaB, RaC and RaC', so information regarding RaA concentrations may be elicited, but with decreased certainty, especially in the presence of a background count.

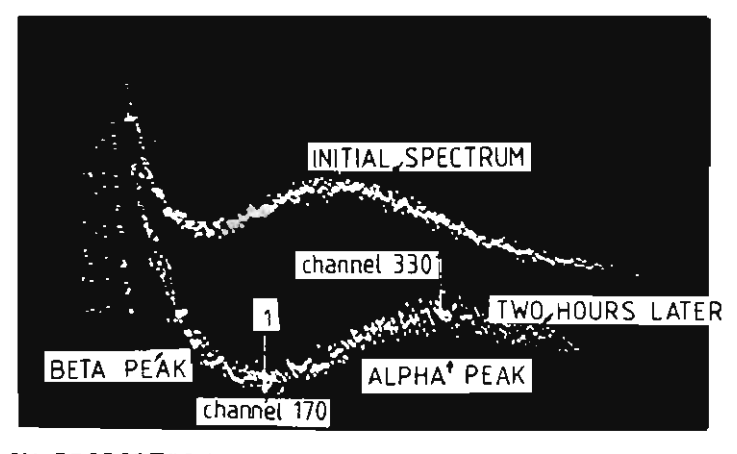
For a given initial number of RaA, RaB, RaC atoms on the filter, a unique set of RaA, RaB, RaC and RaC' decays is predicted, excluding intrinsic statistical fluctuations. The converse also applies - a measure of the number of RaA, RaB, RaC and RaC' decays during a counting period gives information related to the number of RaA, RaB and RaC atoms on the filter. From this the concentrations of each radon daughter and the WL may be determined.

3.2 Feasibility Study

To demonstrate that β - α delayed coincidence could be used to measure RaC, it was desirable to use a detector capable of discriminating α and β radiation.

A gas flow proportional counter (EBERLINE FC-1) was used for this purpose, since β - α energy discrimination, together with a low dead time could be obtained.

The counter was calibrated with a 241 americium source, but a severe problem was revealed that prevented its use past the feasibility stage. The initial flushing of the counter with 'P10' gas (90% Ar, 10% CH₄) produced an acceptable spectra, but the gain increased with time. The spectra below shows the change in gain between a measurement just after an initial flushing period (top) and a couple of hours later (bottom).

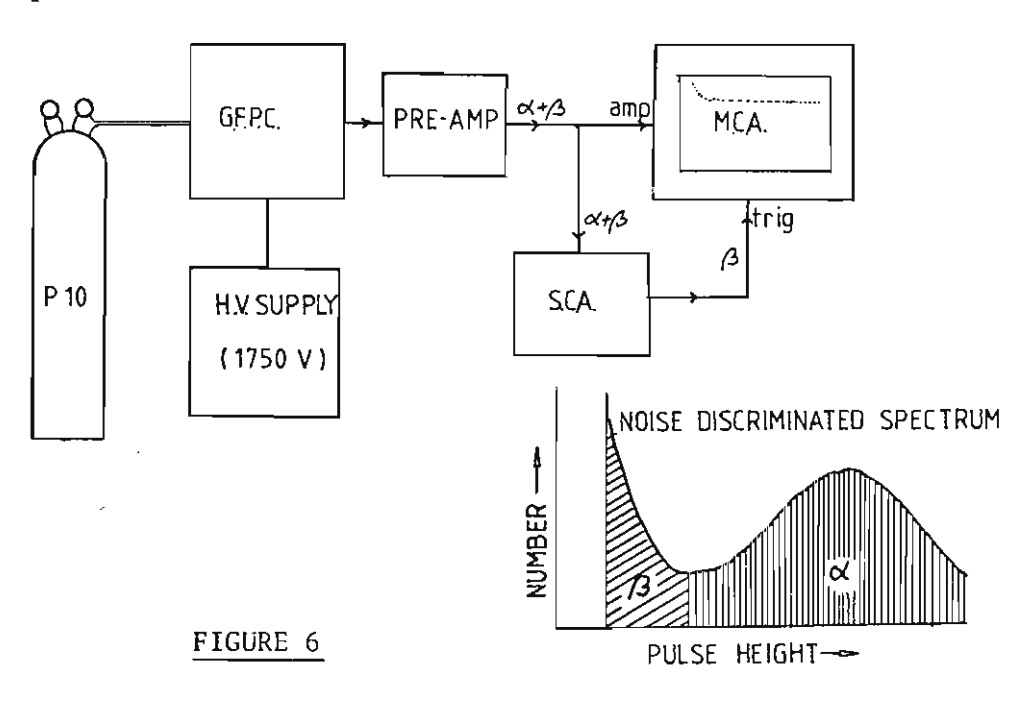


GAS FLOW PROPORTIONAL COUNTER SPECTRUM FOR 241 AMERICIUM

FIGURE 5

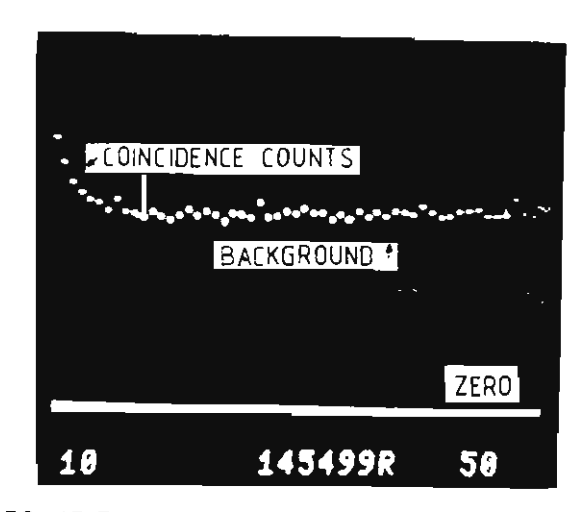
The marker '1' above delineates between the β and α part of the spectrum. It shows a distinct shift from the upper spectrum. A measurement of α radiation based on α - β discrimination would show a false increase in the count attributed to alpha particles as the gain increased with flushing. The reason for this change in gain is the extreme sensitivity of this type of detector to any impurities. Attempts to overcome this problem are discussed in Appendix 9.

To demonstrate that RaC' could be detected by delayed coincidence, the experiment indicated by the block diagram below was performed.



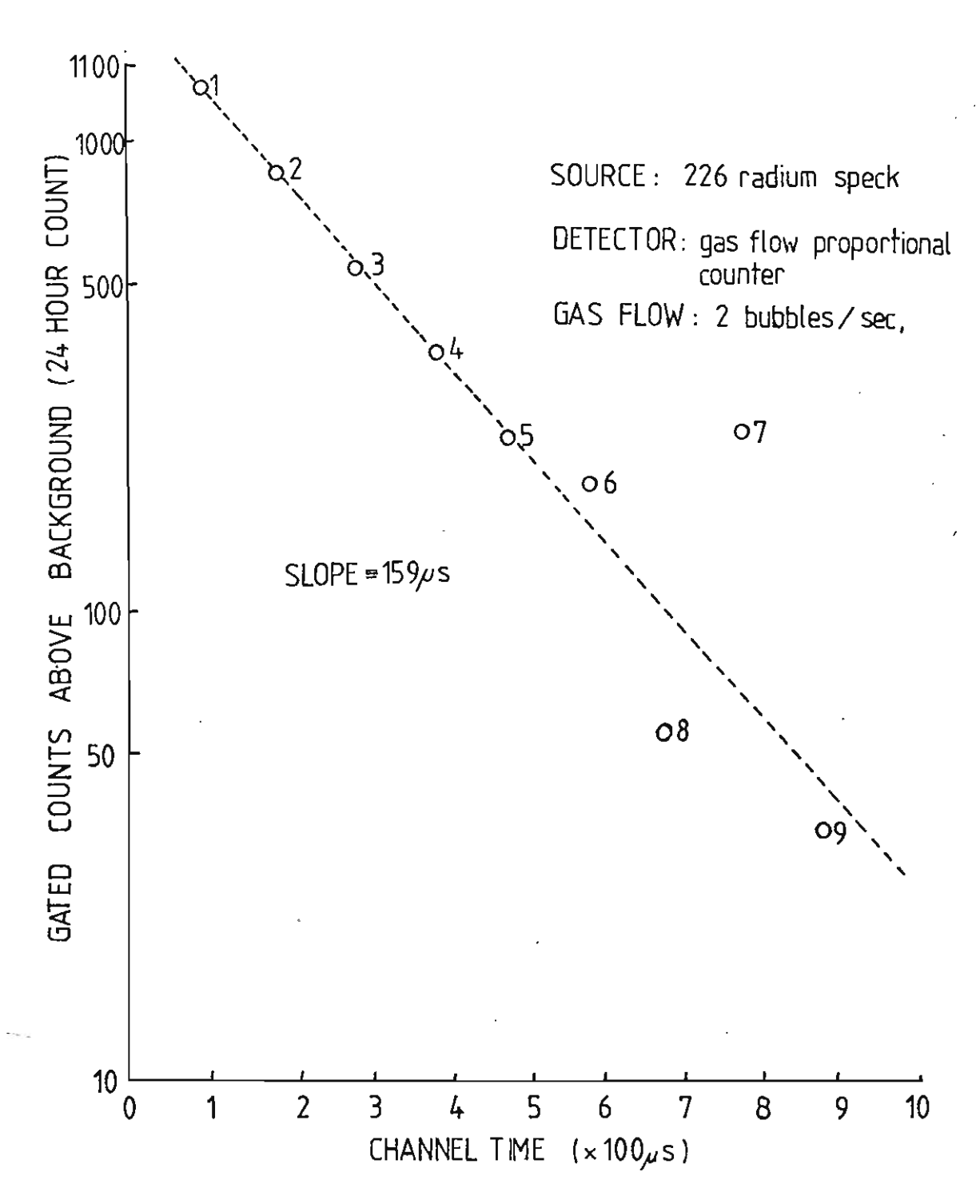
A speck of 226 radium from a luminous badge was glued to a filter and placed in the counter. Though it produced a high radium background, it was felt that sufficient RaC/RaC' would accumulate to be detected, despite the flushing action of the P10 counter gas. The output of the gas flow proportional counter (GFPC) was amplified (Canberra pulse preamplifier model 1406) and fed into the amplifier of the multichannel analyser (Canberra 4100 MCA). The MCA input discriminator was set to count only α particles. The preamplifier output was also discriminated by a single channel analyser (Nuclear Data model ND-520) against noise and α particles and used to trigger the MCA in its

multiscaling mode. In this mode, the MCA is triggered by β radiation and any alpha radiation in the following $100\mu s$ is counted and the total placed in the first MCA channel memory. The MCA automatically increments at $100\mu s$ intervals until its sweep ends, and it awaits another trigger signal. In this way any $\beta\text{-}\alpha$ delayed coincidence counts from RaC/RaC' will produce a discernable decay curve of half life $164\mu s$, on top of a noise count. The display of the MCA is shown below from a 24 hour rum.



COINCIDENCE SPECTRUM - GFPC
FIGURE 7

The average background from channel 10 to 50 was subtracted from the initial decay curve, and the counts in the first few channels plotted on log graph paper (see Figure 8). A least squares fit to the first five data points gave a slope corresponding to a half life of $159\mu s$, while if the sixth

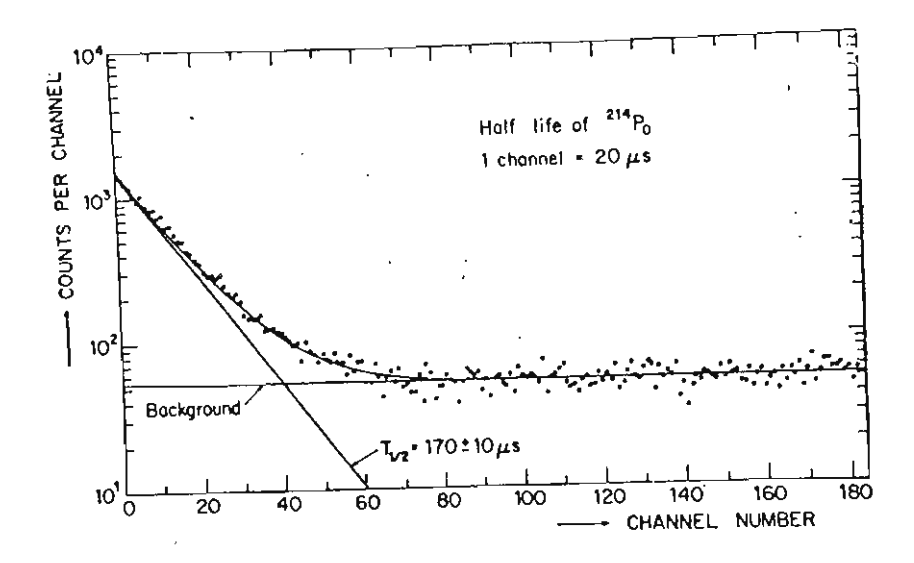


RaC/RaC' COINCIDENCE COUNTS FROM FIGURE 7 FIGURE 8

point is considered, then the result is The of 170µs. The error analysis is complex, but is discussed for a similar measurement in Appendix 10.

Both these compare well with a similar measurement using a multiscaling interval of $20\mu s$ (of $100\mu s$ here) made by ERLICK (1971) using a 230 uranium solution evaporated onto a film and placed between two silicon surface barrier detectors.

The results obtained by ERLICK are shown in Figure 9.



COINCIDENCE DETERMINATION OF Ty2 Rac' after ERLICK (1971)

FIGURE 9

Both results show that RaC' can be positively detected, even in the presence of a high background.

(ERLICK used delayed $\alpha-\alpha$ coincidence between the decay of 218 radon and 214 polonium (RaC') shown in the chain below.

230
U $^{\alpha}$ 226 Th $^{\alpha}$ 222 Ra $^{\alpha}$ 218 Rn $^{\alpha}$ 214 Po $^{\alpha}$ 210 Pb $^{\rightarrow}$ $^{20.8d}$ $^{30.9m}$ 385 $^{0.0355}$ 164 µs 22 y $^{5.991}$ MeV $^{6.45}$ MeV $^{6.68}$ MeV $^{7.26}$ MeV $^{7.835}$ MeV

Silicon surface barrier detectors and alpha spectroscopy were used.)

4. EXPERIMENTAL PROCEDURE

The main purpose of this report is to investigate a new delayed coincidence technique for determining RaC/RaC' in a sample of air containing 222 radon and its daughters. Before describing the detectors, electronics and experimentation associated with the main study, some peripheral investigations will be briefly considered.

4.1 Oil Experiment

A short experiment was devised to investigate the possibilities of using an organic liquid to collect radon from air for liquid scintillation. The collection efficiency was determined by - spectroscopy. The details and results of this experiment are discussed in Appendix 8.

4.2 Two Filter Tube

A simplified two filter tube for simultaneous determination of radon and radon daughters was designed and constructed. Only the first filter was used, but a superior performance of the second filter stage is indicated. The design considerations and working drawings are discussed in Appendix 4.

4.3 Radon Generator

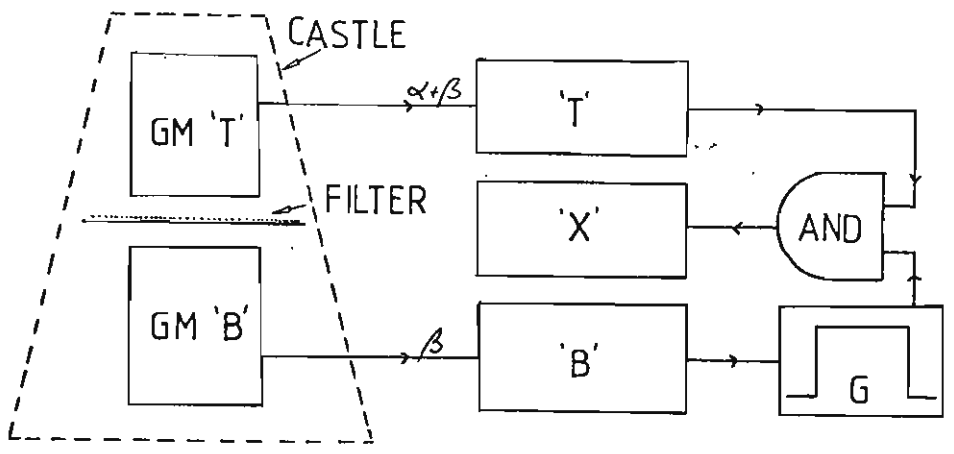
A 250ml "Quickfit" jar was used to contain a 226 radium chloride solution. A "Quickfit" sintered glass bubbler was modified to extend to the bottom of the jar and glass stopcocks fitted to the inlet and outlet, forming a gas tight seal for radon.

The radium chloride solution was made by dissolving a luminous radium badge (0.2MBq, $6\mu\text{Ci}$) in dilute hydrochloric acid in a flask. The phosphor was left as a sediment when the solution (40.1 ml) was transferred to the radon generator several days later.

4.4 The "System"

The concept of the system was discussed briefly in Section 3.1 but is described in more detail here.

Two organically quenched GM tubes (GEC EHM2S) were arranged in a lead castle (Nuclear Enterprises type 710) so that a membrane filter could be placed between them.



BLOCK DIAGRAM OF COINCIDENCE SETUP FIGURE 10

The output of the two GM tubes were placed into identical scalers 'T' and 'B' (ESI Nuclear type 5360). The output of the lower scaler, B triggered a pulse generator 'G' (Intercontinental Instruments Inc. model PG2) which opened an integrated circuit "AND" gate for the predetermined length of its pulse. A pulse from 'T' was recorded by scaler 'X' (ESI Nuclear model 237) when the gate was open.

4.5 Theory of Operation of "System"

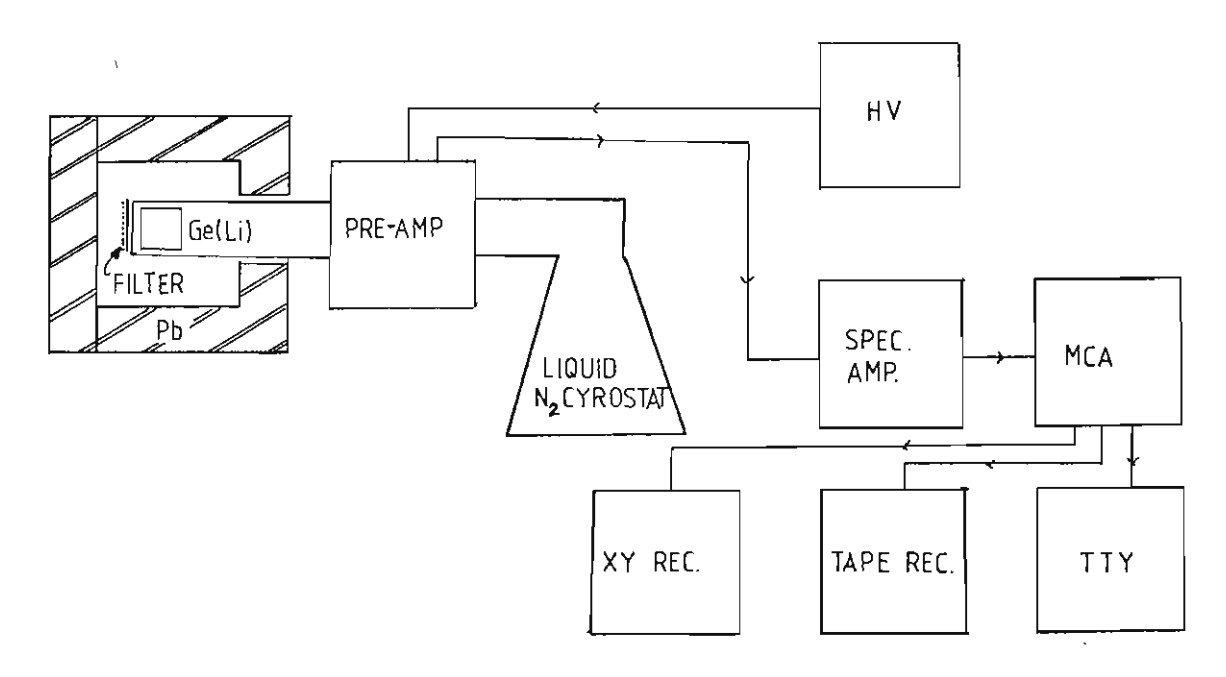
The upper detector 'T' detects both incident α or β radiation. However, since the detector/scaler has an imposed electronic dead time (180µs), only a fraction of the RaC' α 's are counted if they are preceded by a RaC β . Apart from this correction, dead time corrections are minimal at low count rates.

The lower detector 'B' detects only β radiation from RaB and RaC, the alpha radiation being stopped by the combined stopping powers of the filter and detector window.

The delayed coincidence count rate depends on the length of the gating pulse and the activity of RaC on the filter. The mathematics is discussed in Appendix 5.

4.6 Y Ray Spectroscopy

A simultaneous measurement of RaB and RaC was provided by ${f x}$ ray spectroscopy to complement the system measurement. The sensitive portion of a coaxial Li drifted germanium [Ge(Li)] detector (Ortec model OR81) was surrounded by low activity lead and the output placed in a spectroscopy amplifier (Ortec model 472A). A 4kV bias (Ortec mode 559 0-5kV bias supply) was applied to the detector. The output of the amplifier was placed in a 1024 channel multichannel analyser (Norland Intech 5300 MCA). allow sequential spectra to be recorded quickly the data was placed in a small data cassette recorder at the end of each count. The spectra were placed back into the MCA after the run and a numerical output obtained on a teletype printer and a graphical plot on an X-Y recorder produced simultaneously for each spectra. This gave a convenient graphical aid to peak detection and presentation of sequential data. Since the activity of each radon daughter presented to each system was the same, an empirical calibration was possible for RaB, RaC and RaC'. The block diagram illustrates the setup (Figure 11).



 $\frac{\text{FIGURE 11}}{\gamma \text{ ray SPECTROSCOPY OF THE FILTER ACITIVTY}}$

4.7 Experimental Procedure

The filter tube was loaded with filters (Millipore, 0.8μ membrane filters) and connected to the air pump (THOMAS 7A 230V general purpose pump) and radon jar as shown below.

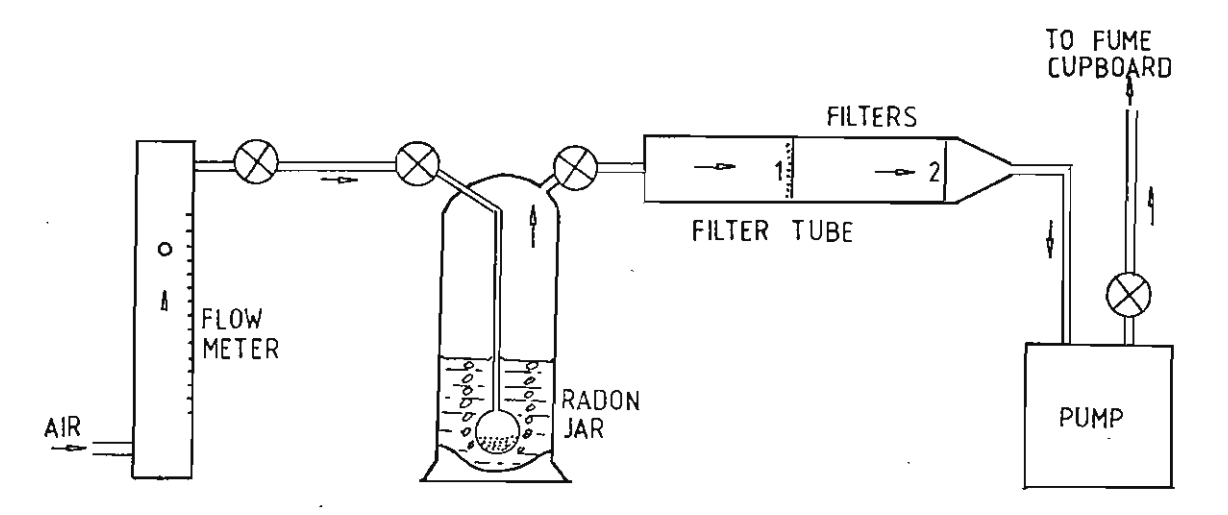


FIGURE 12

COLLECTION OF RADON DAUGHTERS

The flow meter preceded the radon jar to maximise any daughter activity in the air to be filtered. Control of the flow was performed at the pump rather than at the flow meter.

Several stop watches were started when sampling began as a reference time for the γ spectroscopy and system data collection. The radon jar was "de-emanated" for five minutes at 14 1/min. The first filter was removed and cut in half with scissors. One half was placed on the Ge(Li) detector and the other between the two detectors in the GM system with the activity facing upwards. The three runs were performed with the jar undisturbed for 10, 3, and 19 days, so that different degrees of equilibrium between 222 radon and 226 radium would occur. Though most of the daughters were expected to 'plate out' in the jar, it was hoped that some variation in radon daughter concentrations would occur.

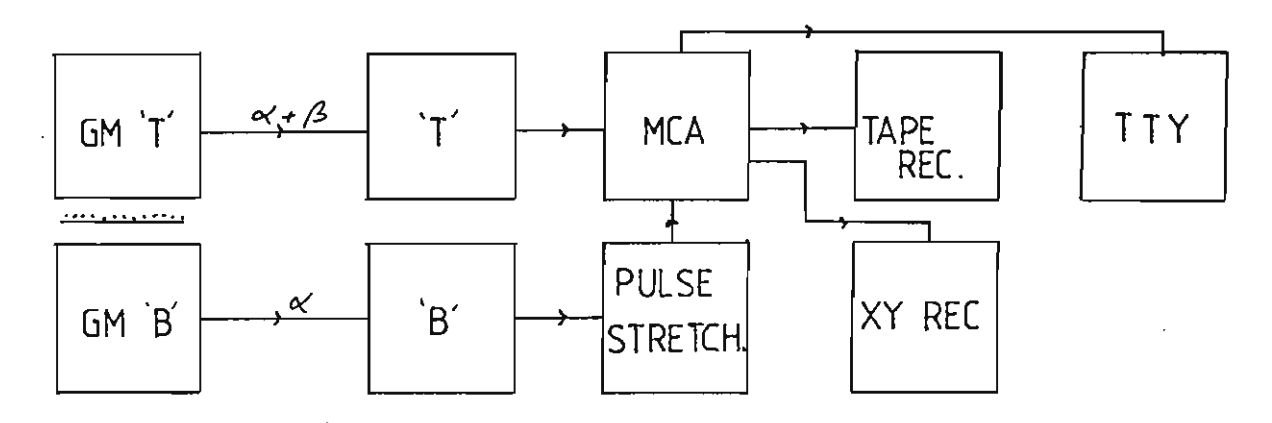
It was found with experience that a geometrically increasing counting periods produced the best results, since the most rapid changes in activity occurred at the beginning of the sequence of counts. The Ge(Li) data was placed on a data cassette whereas the "system" data was recorded as a running total for the three scalers. In addition, a damped chart recording of the T and B scaler ratemeters was recorded (RIKADENKI 2 channel recorder). The coincidence input pulse was stretched and recorded either directly or divided by 10 or 100 and recorded using the recorder event marker. A continuous record of the "system" data was produced.

5. RESULTS

A number of short experiments relevant to the system response were performed. These are described sequentially.

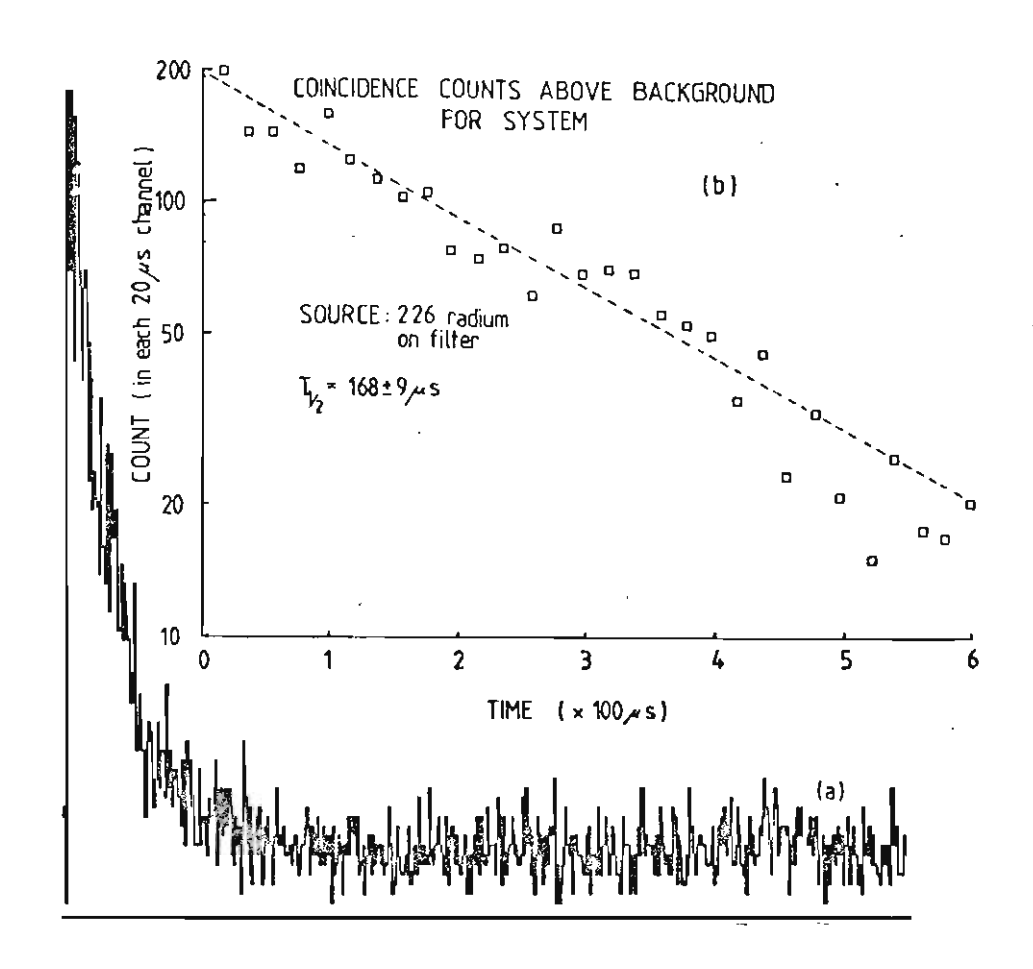
5.1 Multichannel Scaling (MCS)

To demonstrate that the GM-system was capable of detecting RaC' in the coincidence channel, a multiscaling experiment, similar to that in the feasibility study was performed. A new multichannel analyser (NORLAND INOTECH 5300) capable of a dwelltime of 10µs/channel in the MCS mode was used. A pulse stretcher and interface electronics were built to trigger the mode. The following block diagram illustrates the set up.



SYSTEM COINCIDENCE SPECTRUM DETERMINATION

The figure below shows MCS spectra from two overnight runs with a channel width of 10µs per channel.



A Lord Alexander of long layer and relative to the land and the land of the la

GATED TIME SPECTRA OF SYSTEM WITH FILTER
PAPER NORMAL AND INERTED

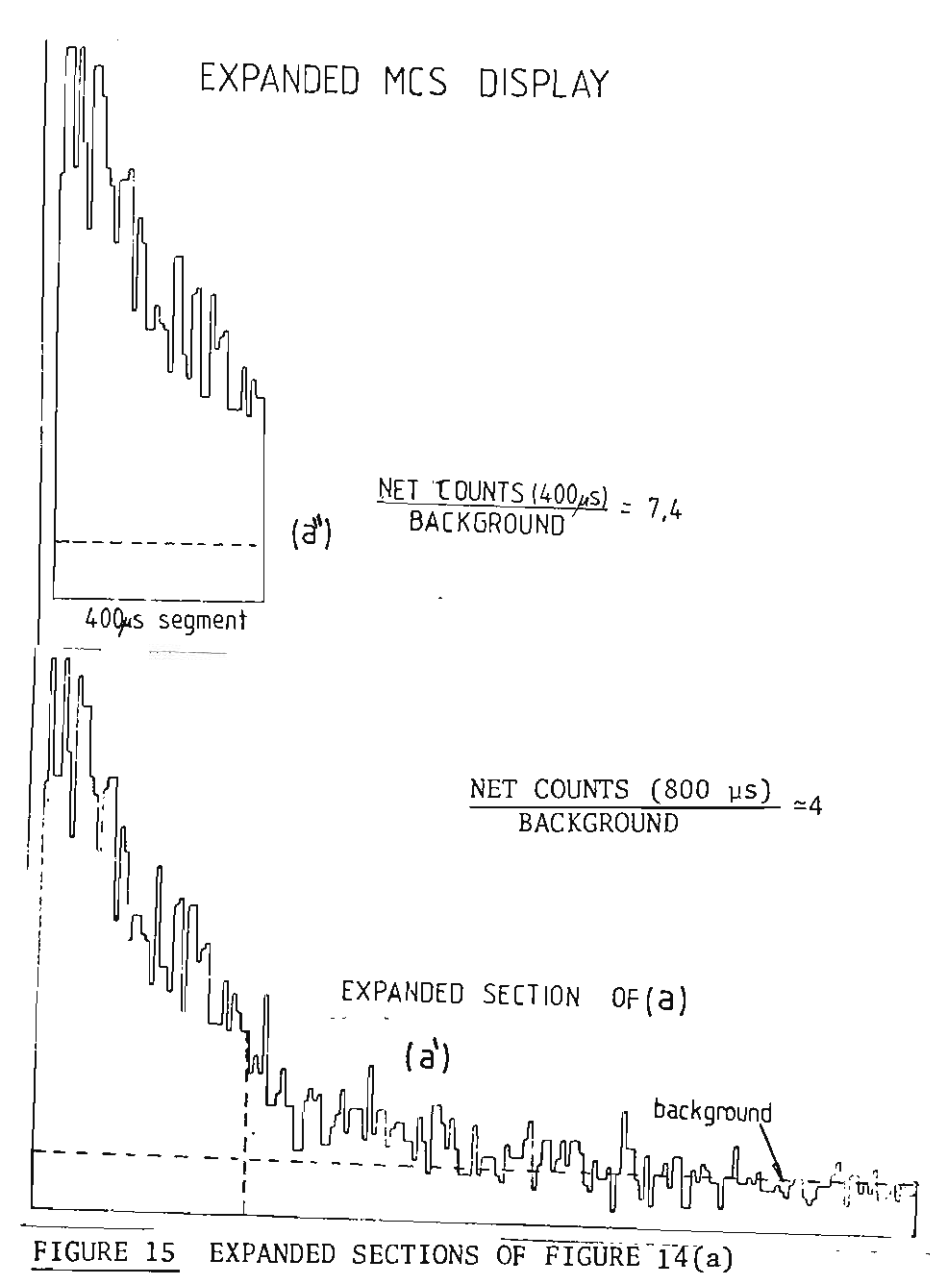
FIGURE 14

The spectrum (a) decays to an average background count of 7.6 counts/channel at longer times. This average background has been subtracted from the first few channels and plotted logarithmically against time (b). The corresponding half life $168 \pm 9 \mu s$ compares well with that obtained by ERLICK(1971) of

 $170\pm10\mu s$ for RaC' by a similar method, but using silicon surface barrier detectors. These results show that after background subtraction the coincidence channel is definitely isotope specific for RaC.

The bottom spectra (c) further proves the efficacy of the system. The source used was a small amount of 226 radium from a luminous radium badge plated onto the top surface of a membrane filter, of the same type used to collect radon daughters. When inverted in the system, the background MCS spectrum (c) was obtained, indicating a total lack of detection of any α radiation from RaC' on the bottom GM since any RaC' detected this way would have produced a spectrum similar to (a). This β specificity is certain, since the range of the RaC' α (7.6 MeV) was greater than any other α radiation (5 MeV) in this decay series. combination of the stopping power of the filter (3 mg/cm²), the air gap and the GM window (2.1 mg/cm²) prevents the detection of any α radiation through the body of the filter. The count on the bottom detector for measuring radon daughters was due to the β radiation from RaB and RaC only (and a negligible γ ray count since these GM tubes were relatively γ insensitive). The implications of this are discussed in section 6.

Part of spectrum (a) from the previous figure is presented on an expanded time base in Figure 15.



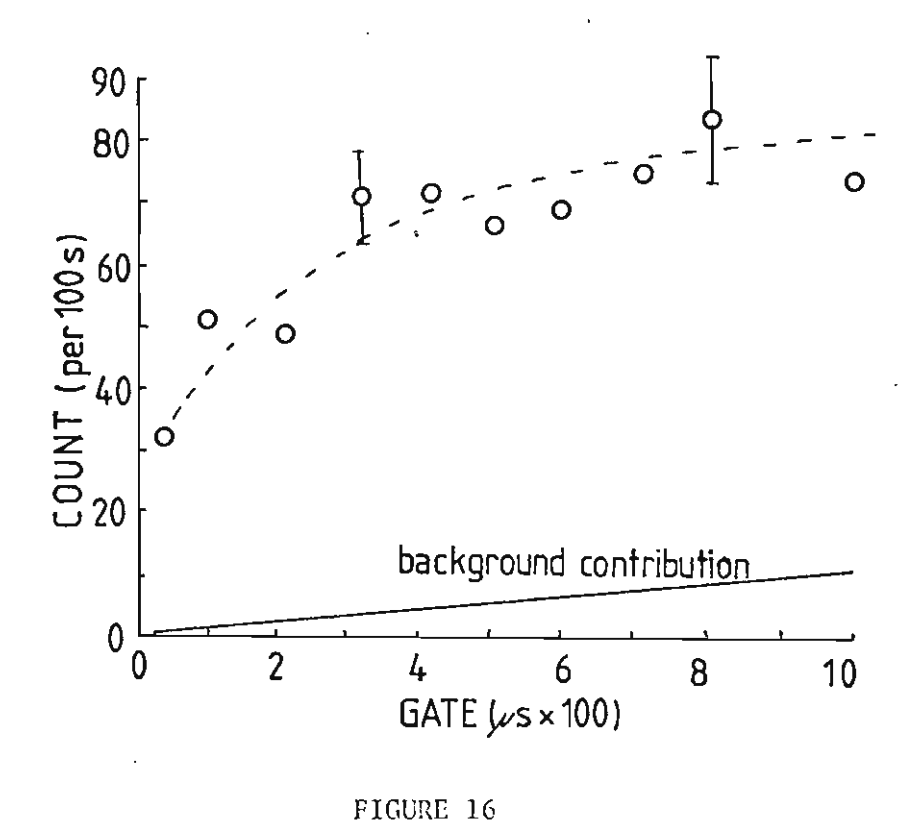
The area of the 40 channel segment (a) represents the total coincidence count obtained when the gate length is $400\mu s$. Spectrum (a') shows the effect of lengthening the gate to increase sensitivity. The gain is offset by the increase in background count.

The spectrum obtained had a greater contribution to background random coincidences than that expected for an environmental sample, since with the 226 radium sources used the top counter registered an equal number of α particles from 226 radium, 222 radon as well as those from RaA (218 polonium) and RaC' (214 polonium). An environmental sample collected on a filter would have an α count contribution from only RaA and RaC'. That the

system performance is good in the present experiment illustrates the degree of background rejection obtained with the coincidence counting mode.

5.2 "System" Gate Optimization

The system was set up in the manner described and the count rate recorded for different gate lengths. The 226 radium source used in the previous section was used.



EFFECT OF GATE LENGTH ON BACKGROUND AND SENSITIVITY

For a gate length G, the possible fraction of RaC' detected is given by

$$F = 1 - e^{-G/\tau}$$

where τ is the mean life of RaC' (236.6 μ s)

GATE (μs)	F(%)
200	57
400	82
œ	100

TABLE 2 DETECTABLE FRACTION OF Rac'

This is shown in the above graph, but an optimisation of the gate length had to be made - too short and the detection lacked sensitivity, too long and the problems of random coincidence counts became evident. A value of 400 μ s was selected as a compromise between high sensitivity and background rejection. The system performance could be slightly enhanced by adjusting the individual channel deal times to the same value of 400 μ s, thus decreasing the random coincidence count since scaler retriggering would not then occur. Measured dead times were between 200 and 250 μ s.

5.3 Channel Dead Time

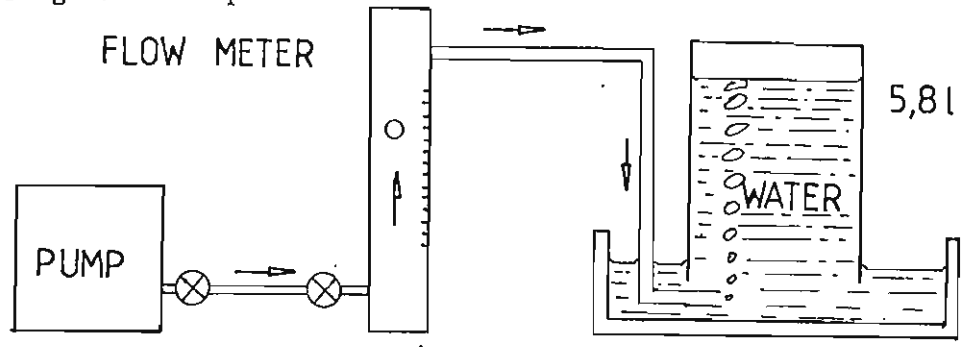
A check on the dead times of the system was performed. The electronic dead time imposed by the scaler was stated to be $400\mu s$, and exceeded the intrinsic GM dead time.

The standard dead time method of split sources was applied (Appendix 12), but two techniques were used. The first involved placing one split source, then the other and then both near the GM tube and calculating the dead time. The count rate was adjusted to produce about 10% dead time with both sources in position, by changing the source-detector distance.

5.4 Flow Meter Calibration

The volumetric flow of air through the filter during sampling in part determines the activity deposited on the filter, so an accurate determination of the flowmeter calibration was needed.

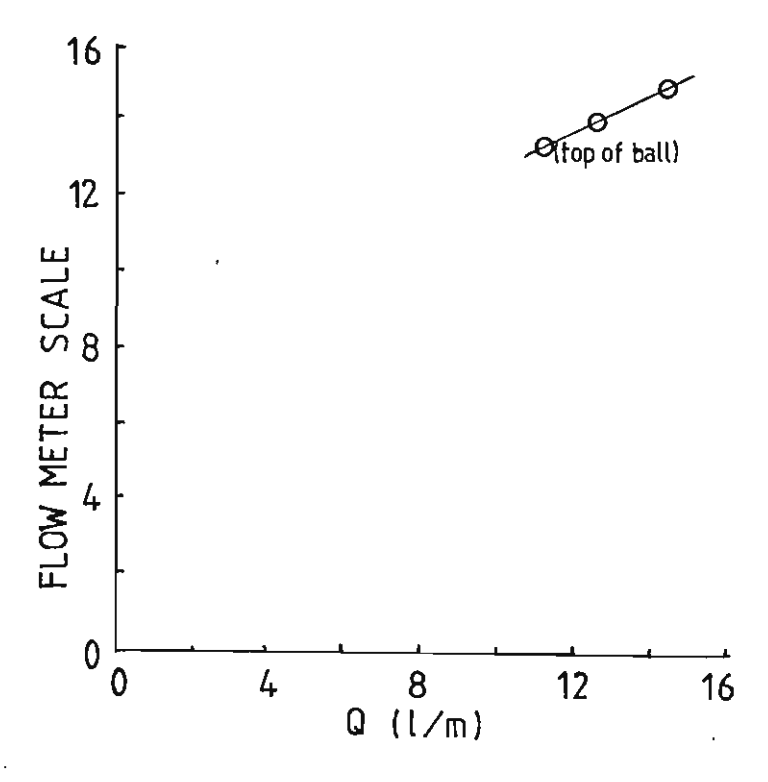
A reasonable calibration at flow rates of interest was performed using water displacement.



FLOWMETER CALIBRATION

FIGURE 18

The flowmeter (FISHER and PORTER TRIFLAT) was of a tapered triangular bore design and lifted a metal ball to various heights depending on the flow rate. No instructions were provided with the meter as to the scale marking or method of reading. The calibration graph below was produced by timing the water displacement from a 5.81 container with a stopwatch.



 $rac{ ext{FIGURE 19}}{ ext{An approximately linear response in the range of interest was found.}$

The second method involved placing both sources near the detector as before, but alternately covering each with a 2mm piece of lead, and then uncovering both for the combined count.

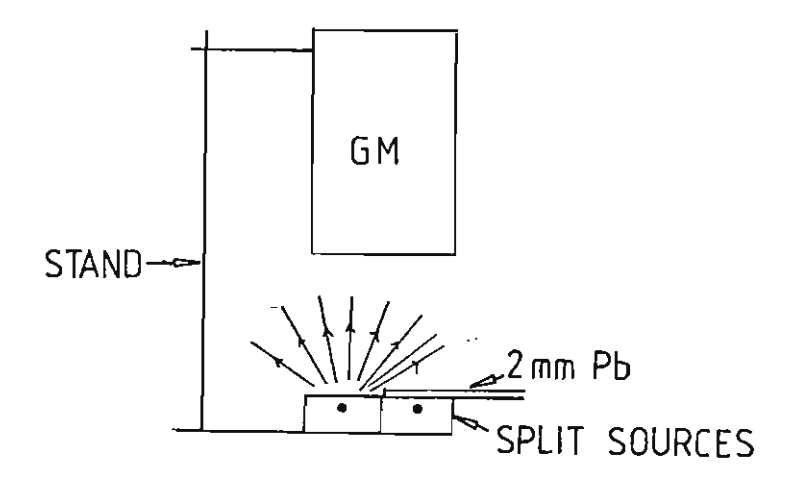


FIGURE 17 GM DEAD TIME DETERMINATION

This avoided moving the sources, but gave a significantly shorter dead time, perhaps due to a small degree of scattering from the lead. The lead reduced the count to background levels when it covered both sources, demonstrating that its shielding effect was adequate. Autoradiography of the split sources showed the active parts to correspond exactly with the 2.5m diameter depressions in their surfaces.

For scalers T and B

	DEADTIME T(μs)	DEADTIME B(µs)
Method 1 (30s count)	200 ± 70	350 ± 80
Method 2 (300s count)	160 ± 20	260 ± 20

TABLE 3

5.5 Results of System Performance

There were seven distinct areas to be considered during testing of the system.

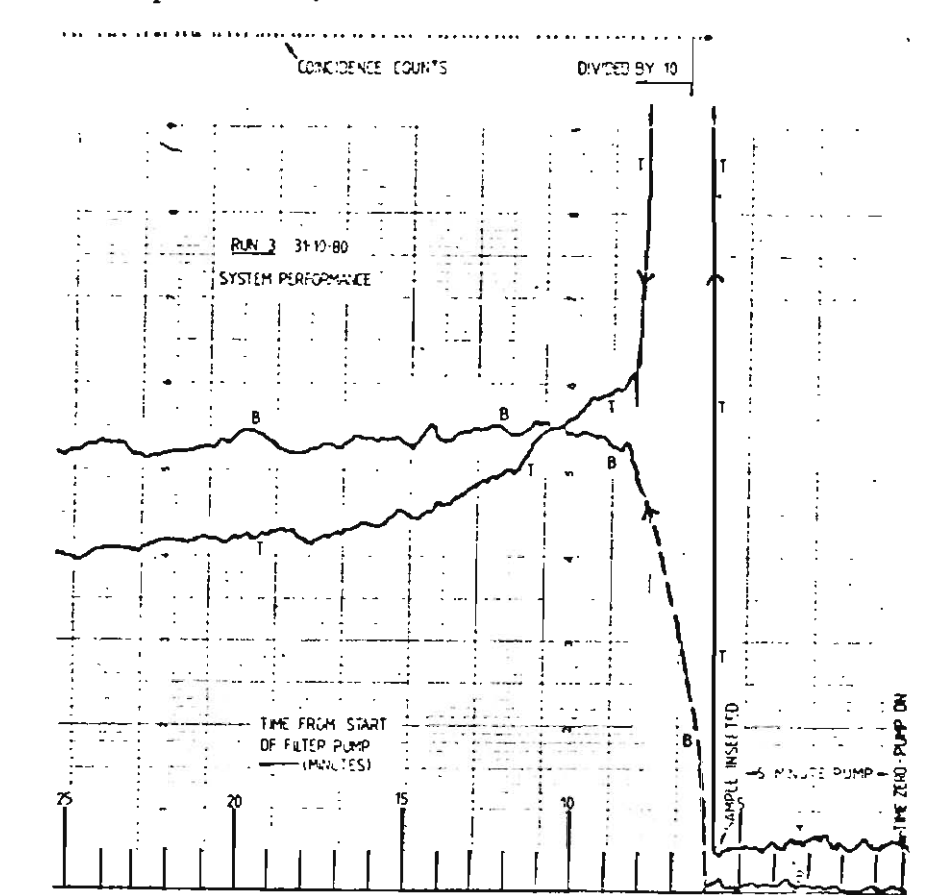
- (1) The dynamic response to radon daughters. Previous tests showed the static response to RaC/RaC' in the presence of 226 radium, 222 radon, RaA and RaB in secular equilibrium but showed nothing of the response to RaA and RaB. This test would also demonstrate the degree of background rejection expected in the presence of radon daughters alone.
- (2) The response of the bottom detector "B" to the presence of RaB and RaC. This could be confirmed by the half lives of the detector counts and by parallel γ spectroscopy of RaB and RaC.
- (3) The ability of the system to indirectly differentiate RaA.
- (4) The coincidence response for RaC/RaC' was repeatable and corresponded to the RaC levels obtained by parallel γ spectroscopy measurements.
- (5) The calibration factors for the system, for each daughter.
- (6) The lower level of detection for each daughter.
- (7) Investigations into measurements necessary to determine RaA, B, C and C' under various conditions.

Three runs were performed with the system and Ge(Li) detector in parallel. The degree of equilibrium of the 222 radon with 226 radium in the radon jar was estimated to be 84%, 42% and 97% for the three runs. Secular equilibrium of the radon daughters with

radon would be expected, so daughter activities in air bubbled through the radon jar should be in the same ratios, assuming the degree of removal of each daughter on each run was the same. This could only be verified to a limited degree since positive identification of only RaB and RaC by γ - spectroscopy could be performed. Examination of the chart recording of the system performance is probably the best indicator of the degree of disequilibrium between the daughters since the transient RaA activity would not be shown as well on an integrated response.

5.5.1 Initial Daughter Equilibrium

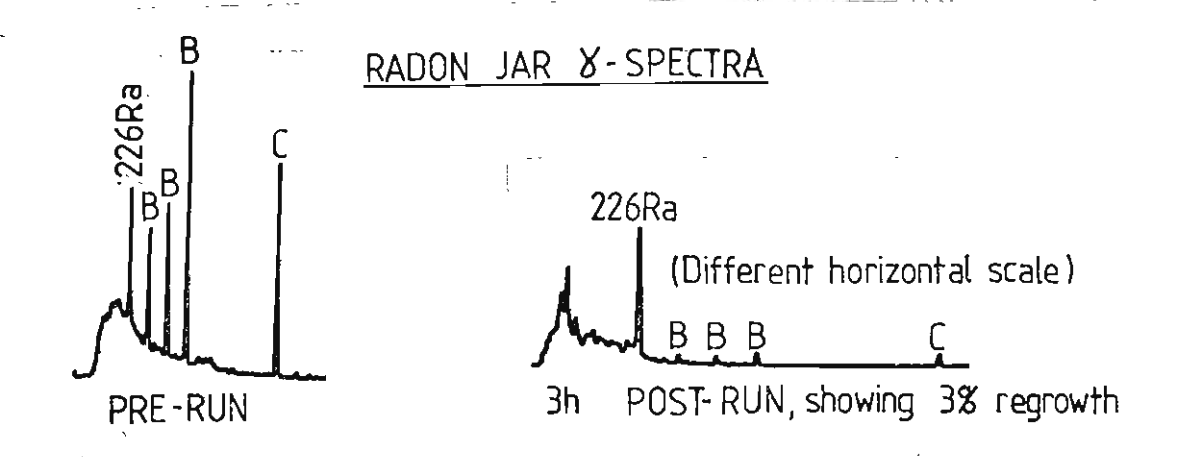
For secular equilibrium between RaA, B and C the activities of the daughters would be the same. For air sampled by filtration, the activity on the filter builds up until the rate of decay of each daughter equals its rate of collection plus its rate of formation. At the end of sampling, the RaA activity decays but the activities of the other daughters follow a more complex process of build up and decay.



The section of the chart recording above shows this feature. The very high (off scale) 'T' trace after the sample was inserted is due almost entirely to the RaA activity indicating a large degree of disequilibrium towards RaA. The gradual buildup and decay shown in channel 'B' is due to the buildup and decay of RaB and RaC. This buildup is also evident in channel 'T' once the dominant RaA activity has decayed. (The dashed line for channel 'B' represents an average value, since several scale changes were hastily made to both channel T and B to allow for the large initial activity in channel 'T'.

The mean life of free RaA (i.e. not attached to condensation nuclei) is about 30s (DUGGAN, 1969). A proportion of RaA was expected to be present in jar air (~10%). A lesser proportion (1%) of RaB and RaC remains free since they were either attached to the jar walls on formation or during their longer half lives. This produced a larger degree of disequilibrium towards RaA on de-emanation.

From γ - spectroscopy measurements of the RaB and RaC activity in the radon before and after a run, an almost complete removal of radon was deduced.



B = RaB

C = RaC

FIGURE 21

This high efficiency (>99%) of removal of the radon suggests that most of the radon and airborne daughter activity had been removed in the first, e.g. 30 seconds of de-emanation. Since this time was unknown, an accurate estimate of the daughter activities on the filter at the *end* of sampling was impossible.

A short discussion of the data from the three runs is presented as a prelude to an assessment of the seven points outlined at the beginning of section 5.5.

For all the runs a sampling time of 5 minutes at 14 1/minute was used.

5.5.2 Run 1 Data

(i) Ge(Li) data (Run 1)

To capture the changes in high initial activity on the filter, the first 500s were recorded in the MCS mode with a channel width of ls. Due to a technical fault in the tape recording this data was lost. Consequently, the γ ray spectra did not show the initial high activity. The form of the spectra is shown below.

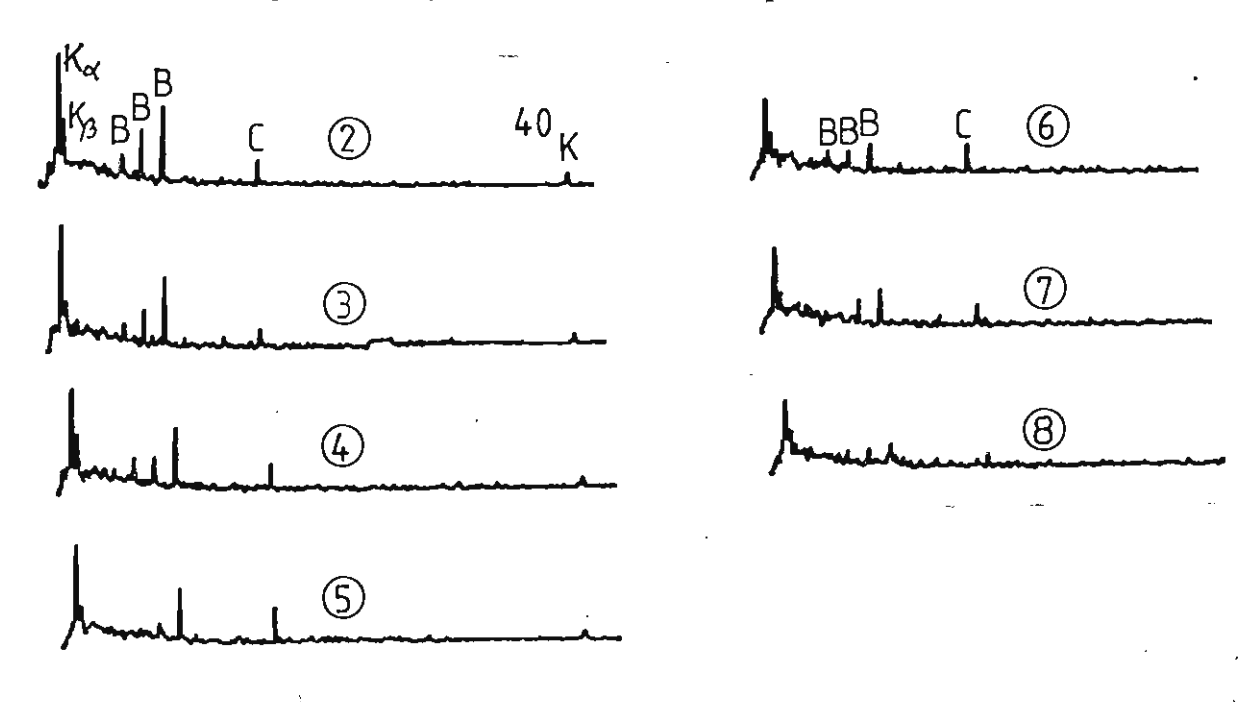


FIGURE 22

RUN 1, SEQUENTIAL γ ray SPECTRA OF FILTER (400s)

The peaks labelled α and β are the lead emission lines from the shielding. The peaks marked 'B' are the RaB γ peaks of 242, 295 and 352 keV.

The peak marked C is the 609 keV γ ray from RaC. Note the decay of RaB and buildup and decay of RaC. Where a slight gain shift has occurred, the counts may be shared over a different number of channels, changing the apparent peak heights.

The data from the γ - spectroscopy can be shown quantitatively by plotting the count rate (peak area/count time) against elapsed time. The plot below shows the decay of RaB for the 297 and 352 keV activity and the RaC 609 keV activity.

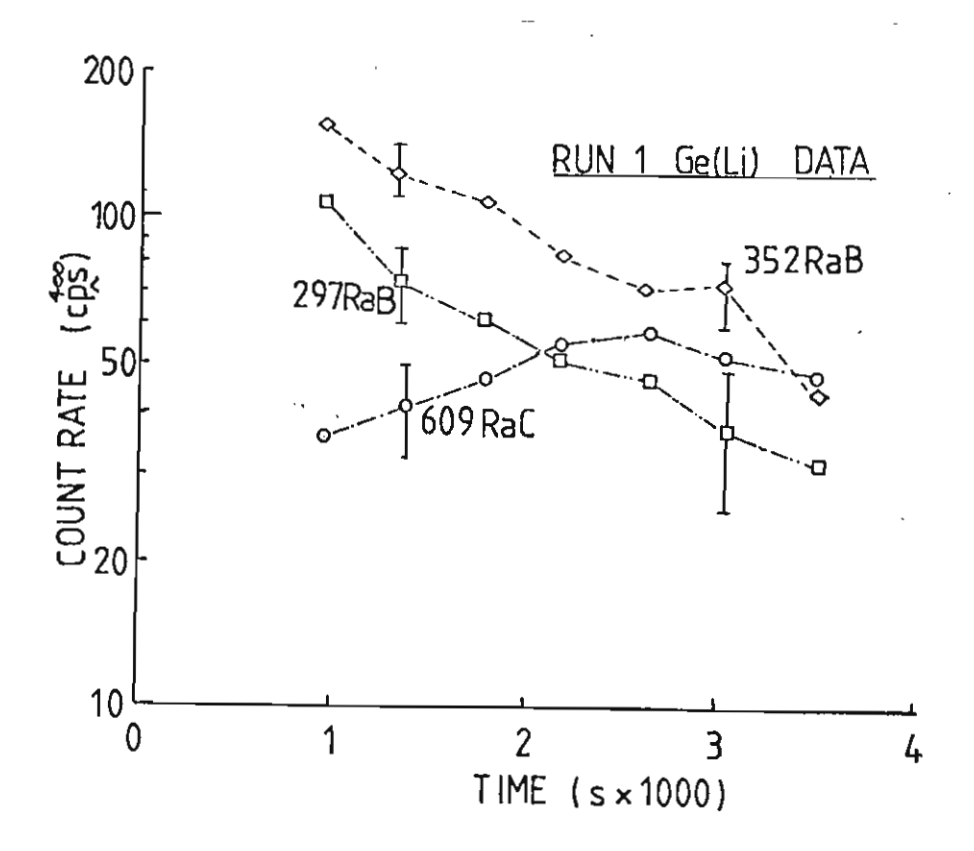


FIGURE 23 RUN 1 RaB AND RaC ACTIVITY BY Y RAY SPECTROSCOPY

The change of activity of RaB and RaC is more evident here than in the set of spectra presented for Run 1.

(ii) System data (Run 1)

The gate interval was set at 200µs and the filter paper placed between the GM tubes. A good counting geometry was ensured by clamping the two GM tubes together. The record for ~three hours (10000 seconds) is shown.

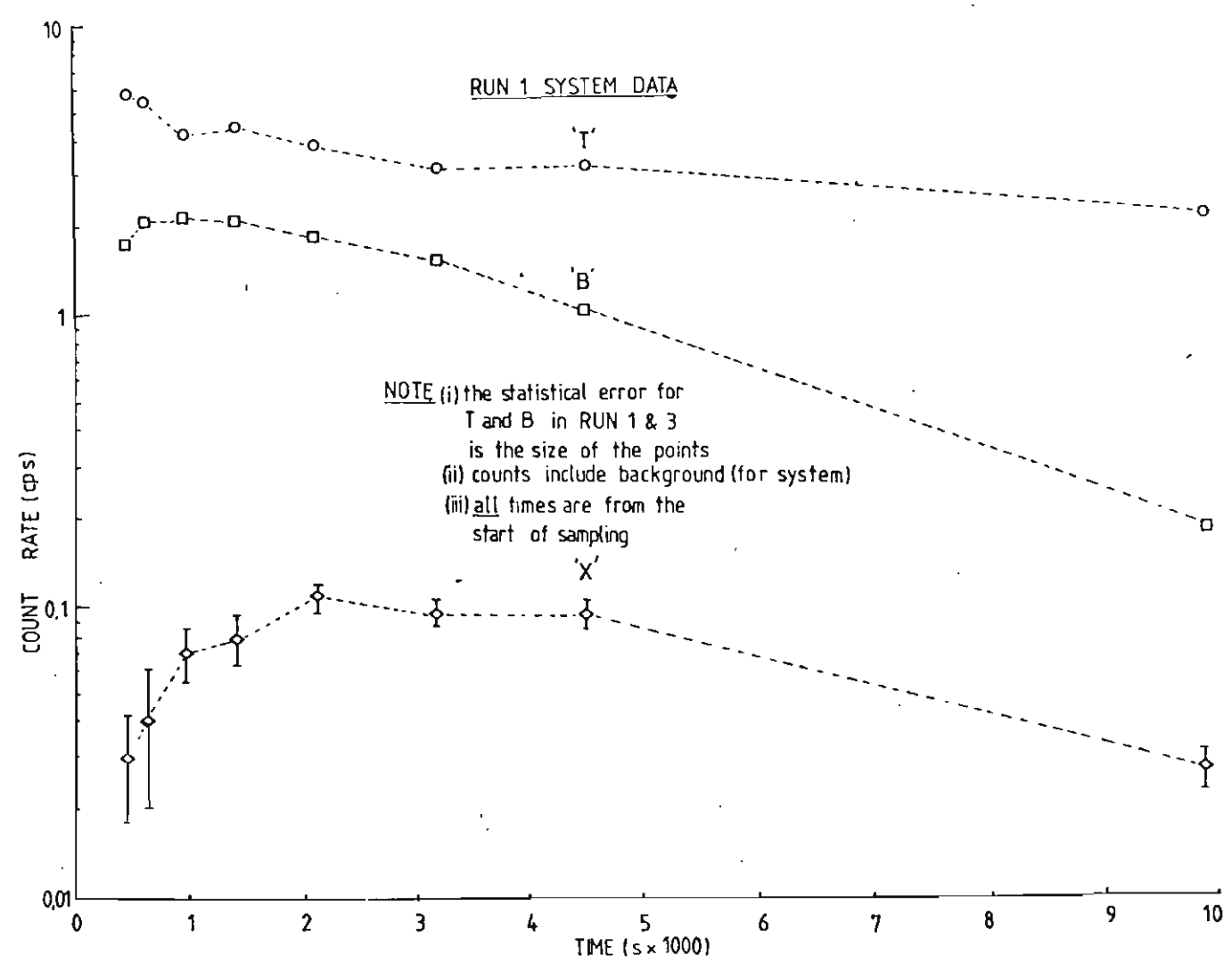


FIGURE 24 RUN 1, CHANNEL T, B AND X RESPONSE

The expected buildup and decay of RaC' is reflected in the bottom curve of similar shape to the RaC curve in the Ge(li) results shown earlier.

The T channel shows an initial high activity from RaA decay and the B channel shows an initial buildup and then a decay. The residual activity in the T, B and X channel was due to gross contamination of the castle with radon gas from a previous measurement.

The resultant daughter activity on the GM tubes, especially the poorly ventilated top GM tube gave a background rate close to the final count rates shown.

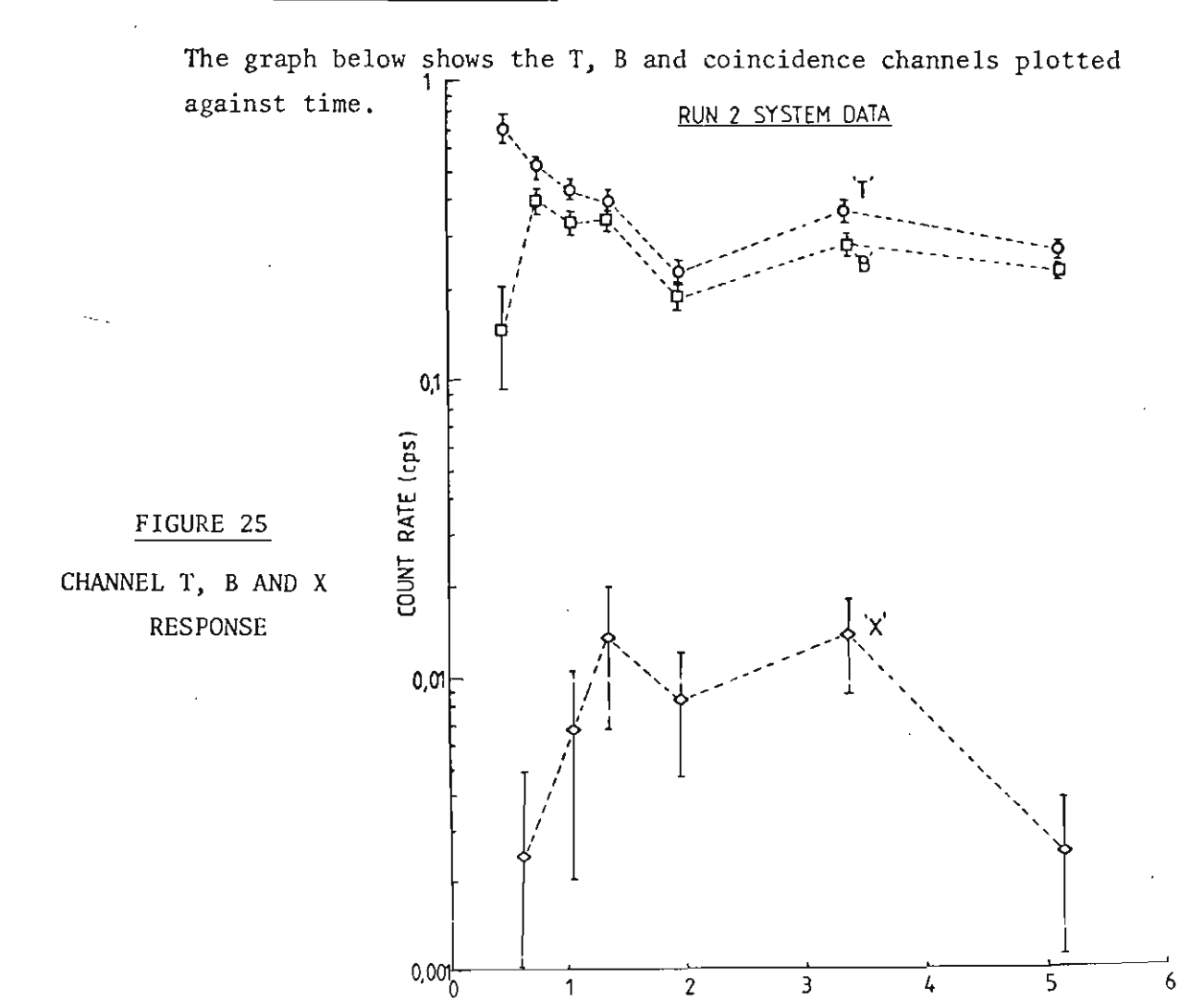
5.5.3 Run 2 Data

The degree of equilibrium of radon in the jar was about 42%, so half the daughter activity in Run 1 was expected. A gate length of $400\mu s$ was used.

(i) Ge(Li) data (Run 2)

The levels of radon daughters were so low that the daughter activity did not show above background.

(ii) System data (Run 2)



A similar result to Run 1 was obtained except the measurements were stopped after 1^{1} hours. Although γ ray spectroscopy could not give any information on the daughter concentration, comparison of the graph above with the system graph for Run 1 shows a *ten*fold reduction in count rate for all three channels and not the twofold reduction expected. The reason for this is not known.

5.5.4 Run 3 Data

Experience obtained from the previous two runs permitted optimisation of count periods so that this was by far the most successful run. The degree of equilibrium (97%) ensured a high initial activity. All the scalers and chart recorders were turned on before the start of pumping so that they were operational when the filter was inserted between the GM tubes, but an uncertainty in this time made the first count after 100 seconds uncertain, so it was not used. A gate length of 400µs was used.

(i) Ge(li) Data (Run 3)

The data below is similar to the data in Run 1, but the buildup and decay of RaC is much more dramatic.

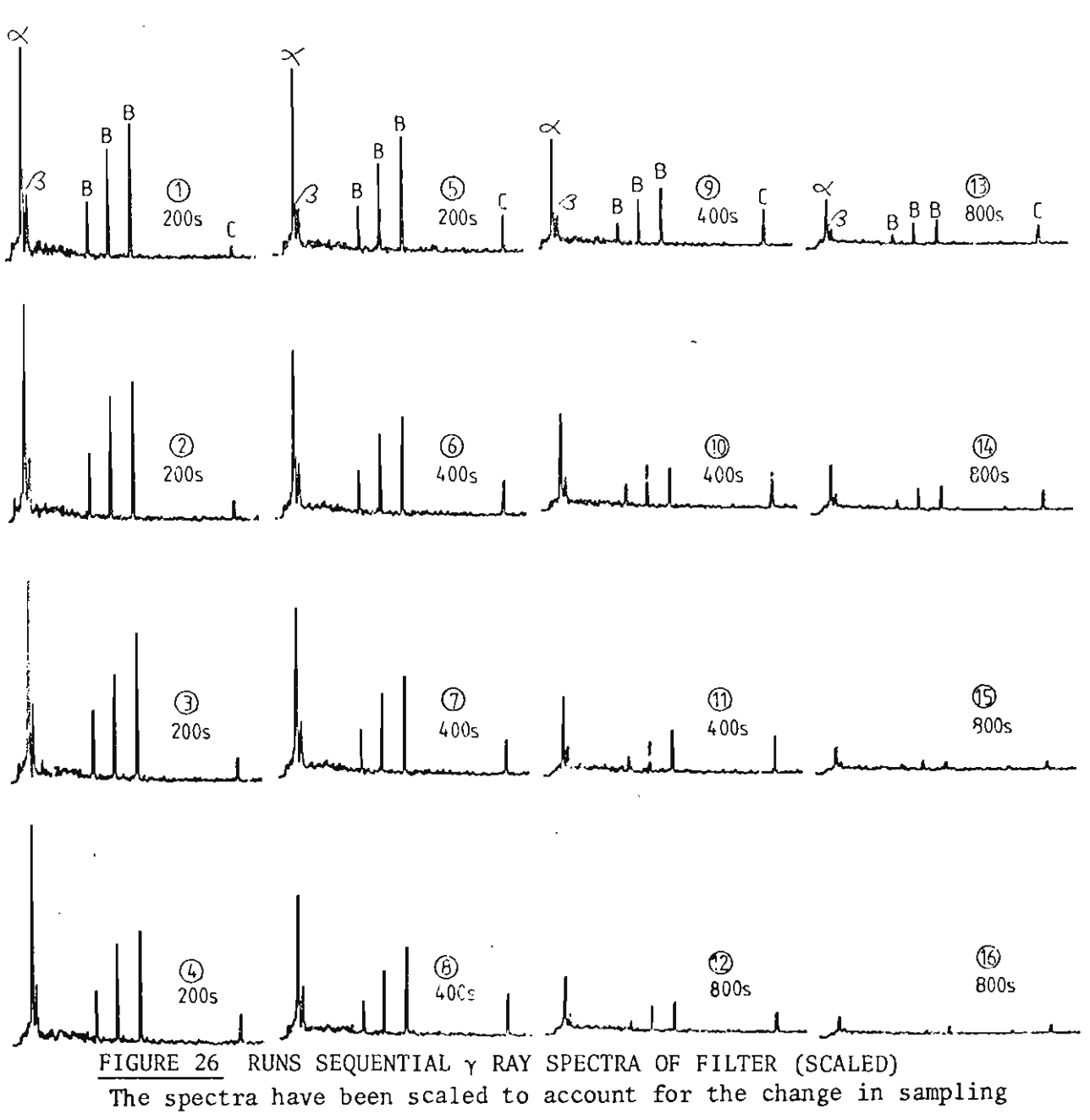
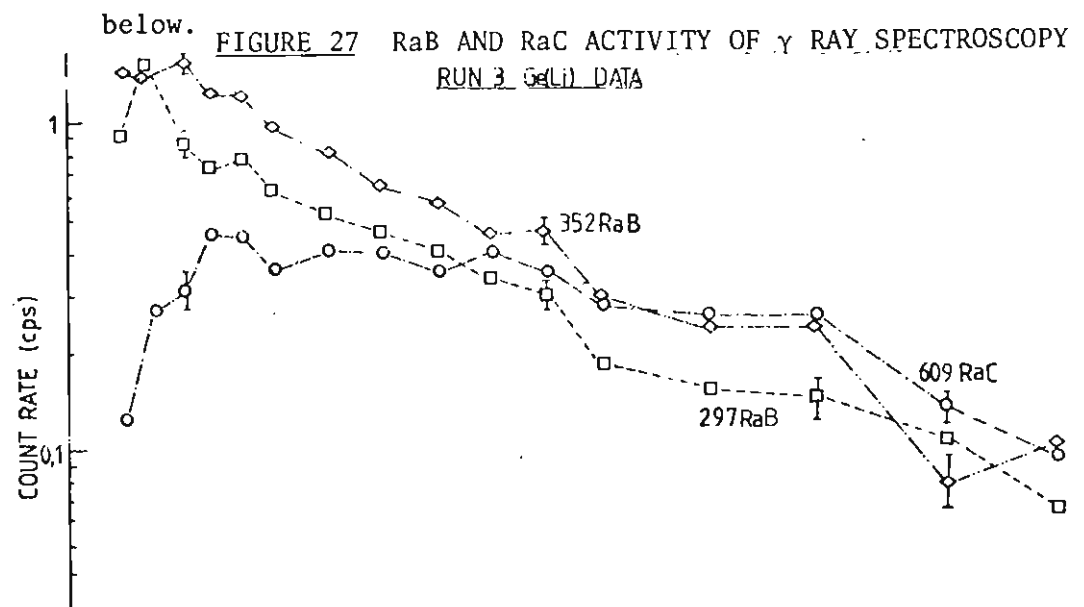


FIGURE 26 RUNS SEQUENTIAL γ RAY SPECTRA OF FILTER (SCALED)

The spectra have been scaled to account for the change in sampling period as the experiment progressed. The changes are plotted below. FIGURE 27 Par AND Page ACTIVITY OF ** PAY SPECTROSCOPY



[ii] System Data [Run 3]

The system data is plotted below. The difference between the position of the T plot here and in Run 1 and Run 2 is due to an accidental change in geometry prior to the run.

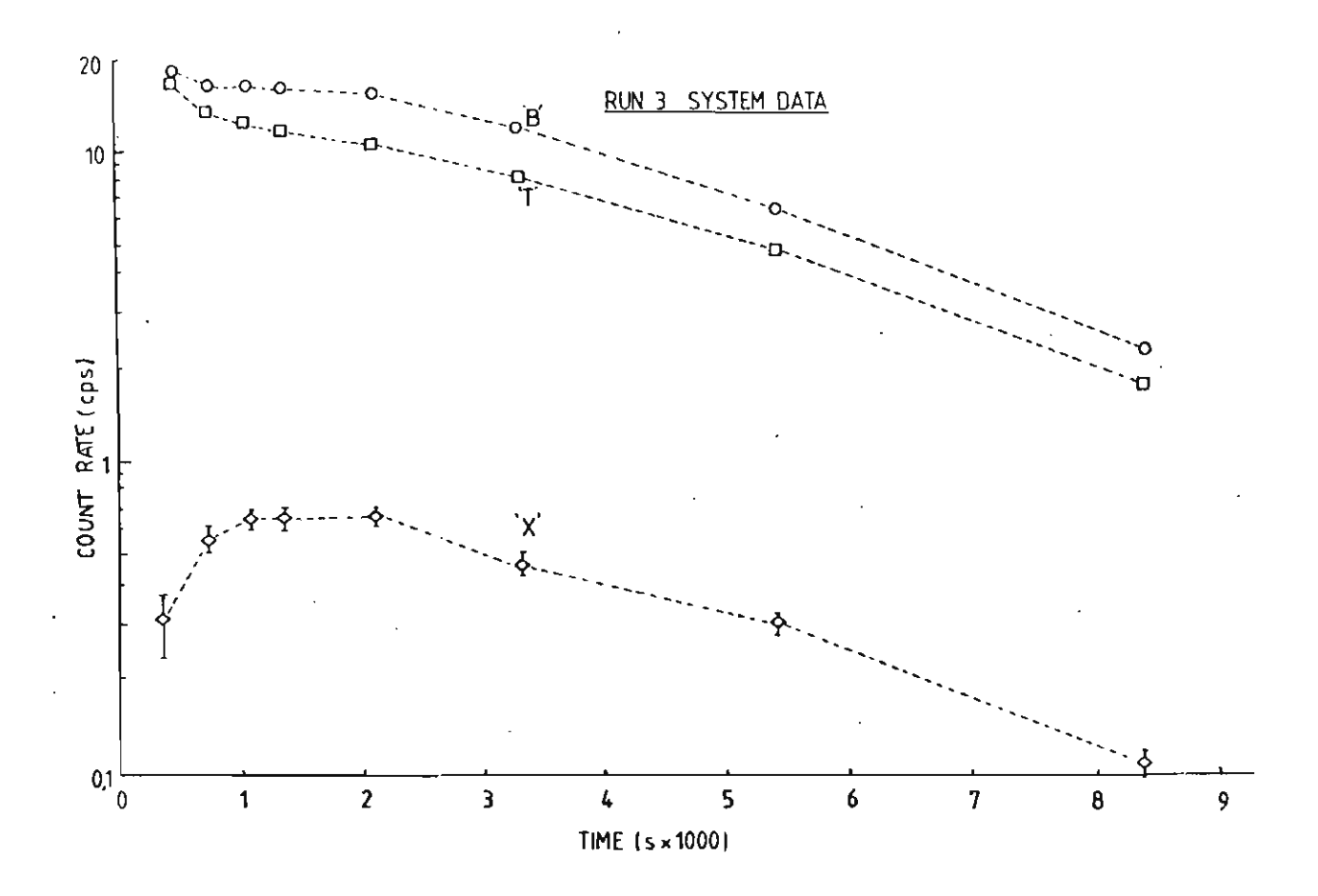


FIGURE 28 RUN 3, CHANNEL T, B AND X RESPONSE

The daughter activity is about fives times higher here than in Run 1. This gives a range in activity.

RUN 1 : RUN 2 : RUN 3 ÷ 10 : 1 : 50

5.6 Analysis of Data

The analysis of the system data is presented under the seven points outlined in section 5.5.

5.6.1 Dynamic Response

The response of the T and B channels can be viewed in terms of decay of RaA, B, Cand C¹. A mathematical treatment of the Run 3 data is given in Appendix 5, but was only partially successful because of a lack of empirical data on efficiencies. This would have required the construction of a high quality thin source to test the data.

On analysis of the Run 3 system data, it was noted that the initial decay of the top counter corresponds to a half life of about three minutes, the half life of RaA. Thereafter, there was a gradual change in the slope of both B and T corresponding to a half life of the sum of the half lives of RaB and RaC, and eventually a decay tending towards the half life of RaB.

5.6.2 RaB Evaluation

A plot of the sum of the Ge(Li) RaC and RaB response gives a similar response to channel B.

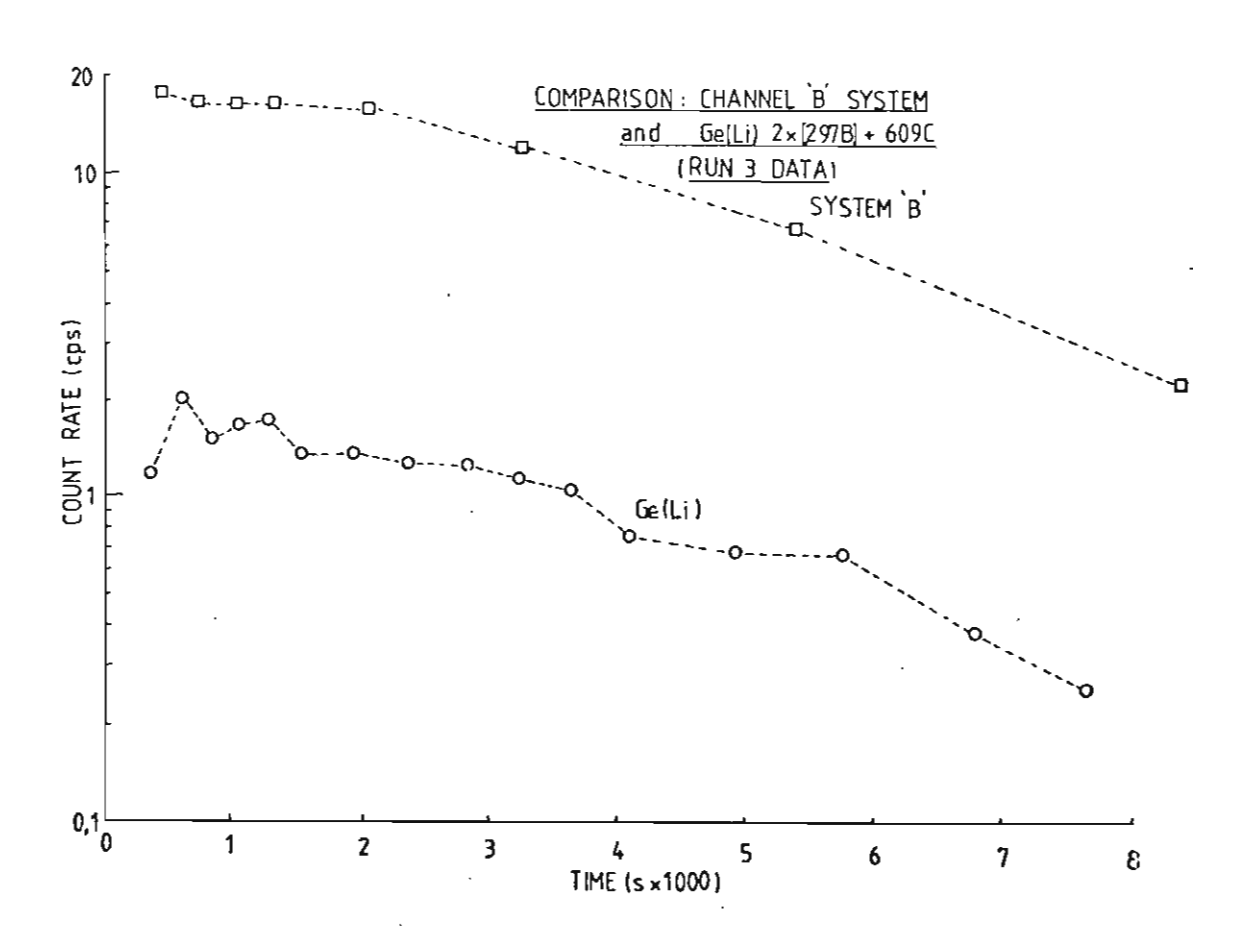


FIGURE 29 RUN 3, CHANNEL B AND COMBINED RaB AND RaC MEASUREMENTS BY Y RAY SPECTROSCOPY

This indicates that the RaB information can be retrieved from the system if the RaC (or RaC') activities are known. The plot of the RaC activity of the Ge(Li) detector and the coincidence channel of the system below indicate this is so.

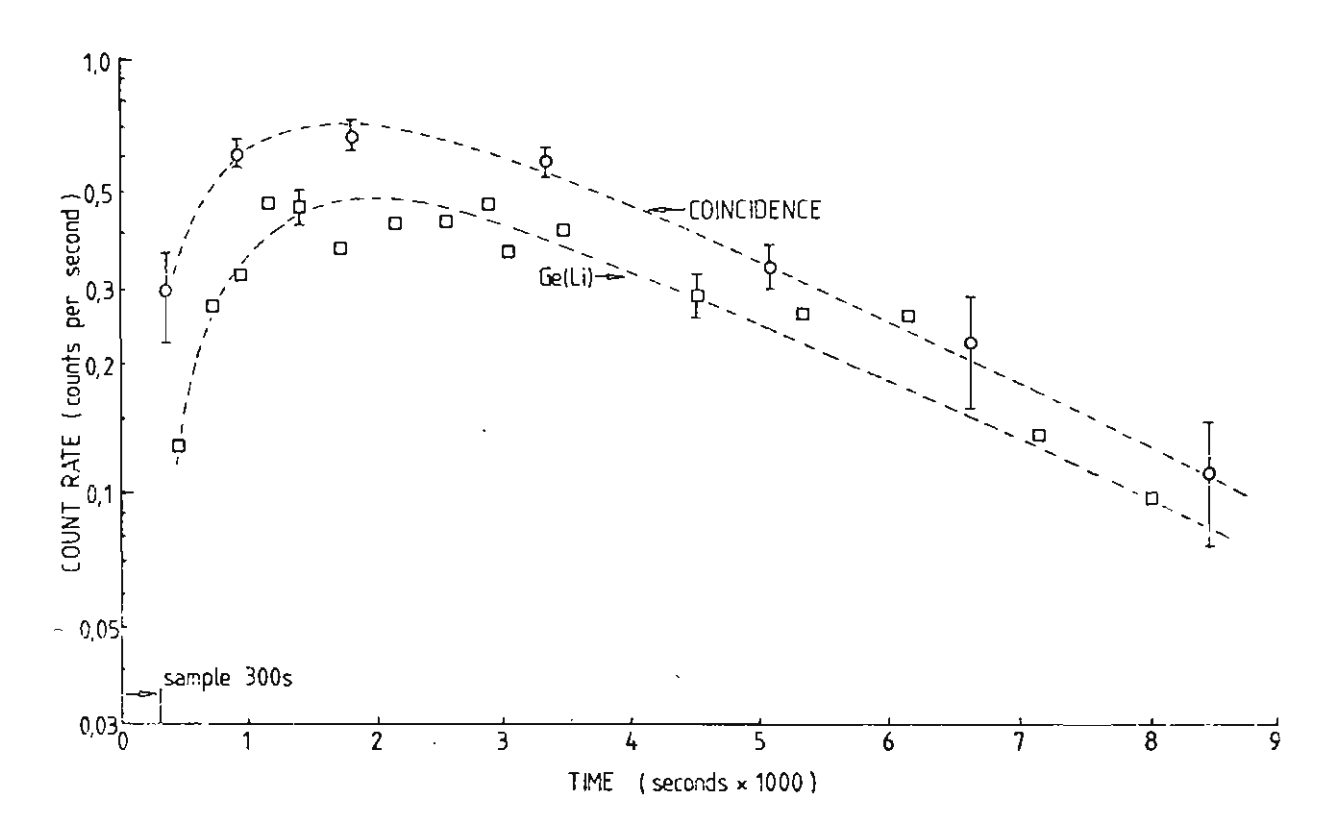


FIGURE 30 RUN 3, COMPARISON OF COINCIDENCE CHANNEL X AND RAC (609 keV)

5.6.3 RaA Assessment

Since the change in RaB concentration with time during sampling was unknown, and the time before measurement was long relative to the half life of RaA (3.05 min), little certainty can be placed on any calculation of RaA activity in the aspirated air. The chart recording in section 5.5.1, as mentioned, showed a very high initial activity of RaA. This was also shown, to a lesser extent in the presentation of the system data for Run 2 and Run 3, since the high initial count rate has been smoothed by the counting interval.

5.6.4 Coincidence Count Repeatability

The shape of the system coincidence channel output in the previous figure matched the RaC Ge(Li) response. Both the Run I and Run 2 coincidence plots were of a similar shape to the Run 3 plot and were both the same proportion of the other spectra.

5.6.5 Calibration

 γ - spectroscopy was used to give total RaB and RaC activity on the half filter presented to the Ge(Li) detector. An error of 3% from bisection of the filter was calculated, so the activity on the filter presented to the 'system' was otherwise identical. The Ge(Li) crystal was approximated to a 46mm disc, 5mm behind the front window of the detector to calculate the geometric efficiency (0.4). The efficiency calibration for a similar detector is shown below.

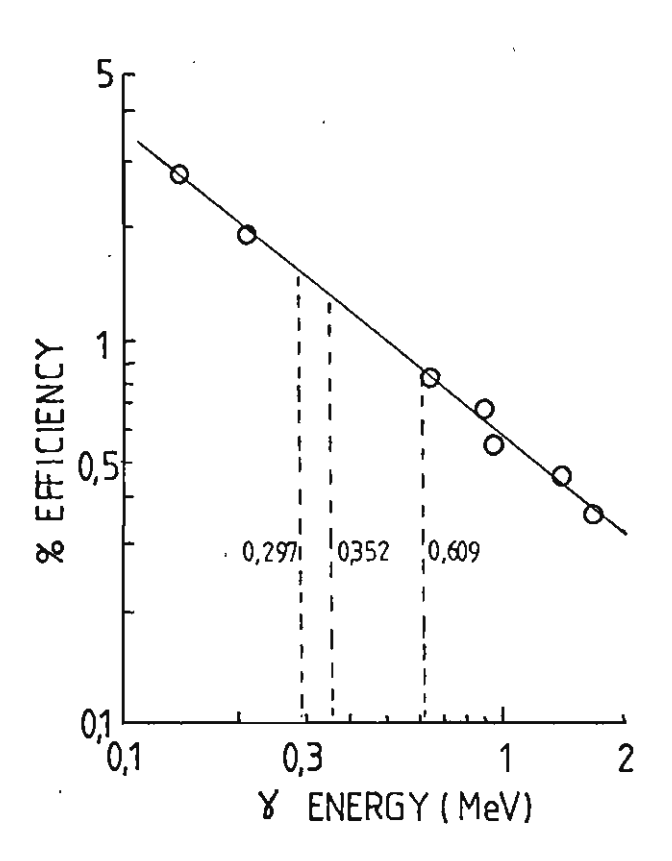


FIGURE 31 Ge(Li) DETECTOR ENERGY CALIBRATION

The count rate ratio between RaC by γ spectroscopy and the system coincidence count was 0.7. The absolute relation between atoms of RaC decaying and RaC γ 's detected gave

312 Bq = 1 count/sec for RaC which translated to

233 Bq = 1 count/sec for RaC/RaC' coincidence counts.

The detection efficiency of RaB and RaC ß radiation by GM is virtually the same, so the detection efficiency of RaB plus RaC towards the end of the runs when secular equilibrium is nearly established can be used to calculate their detection efficiencies. The average ratio of channel B count rate to the coincidence count rate was 25, so the detection efficiency for was

20 Bq = 1 count for RaB plus RaC

A similar detection efficiency for RaA would be expected, since the same geometry was used and the window thickness (2.1mg/cm^2) for the GM tubes used is less than the range of RaA α emissions.

The overal efficiencies may be expressed as percentages

RaA ~10% in channel T

RaB ~10% in both channel

RaC ~10% T and B

RaC/RaC' 0.4% in channel X

The low efficiencies for the prototype were due mainly to the GM window area to the filter paper ratio (~4).

5.6.6 Lower Level of Detection

A mathematical technique for determining the lower limit of detection for a counter is described by ALTSHULER (1953) using an optimisation between type I and type II errors. This is not applicable for the coincidence counting, since the limiting factor is the count time. Extended (1000s) counts of the random coincidence with an unused filter rarely registered a single count. If the mathematics is considered, this may be understood. If the bottom counter B opens the gate G during a count of t minutes, then the fraction of time available for counts from the top counter is $\frac{BG}{t}$ at low count rates. The expected count due to random coincidence 'E' is simply (see Appendix 5).

$$E = \frac{TBG}{t}$$

For example, if the background count rate is 6cpm, for T and B, then the expected random coincidence background using a $400\mu s$ gate during a 20 minute count is 0.0048.

An average background count rate in both detectors of 60cpm was measured to give E \doteqdot 0.5. This may be interpreted as an even chance of registering one count.

If 2×10^{-4} WL air in secular equilibrium is measured in an instrument with detector and filter the same size then (for geometry 0.4, detection efficiency for α and β = 1, sampling 10 1/min for five minutes, counting for 20 minutes (with a one minute sample insertion time) then the counts recorded in the absence of background in channel T, B and X are

38 counts in the top channel, T
32 counts in the bottom channel, B
1.4 counts in the coincidence channel, X.

Doubling of the background rejection may be obtained for a 30% decrease in sensitivity by reducing the gate length to $200\mu s$.

For a background count rate of 6 cps, the effect on channel X is negligible. For the prototype system, the lower limit of detection is 10^{-3} WL, based on the expectation of a single count For an optimized system (larger GM tube or smaller filter), the lower limit of detection would be 2 x 10^{-4} WL.

5.6.7 Measurement of Individual Daughters to Determine WL

Three ways of using the coincidence count to obtain useful information are shown and their merits discussed. A method of estimating the degree of disequilibrium is also presented.

5.6.7.1 Individual Daughters

If the approximate detection efficiencies for RaA, RaB, RaC and RaC' are used, then the individual total disintegrations during the counting interval may be calculated. There is a one-to-one relation between these figures and the airborne concentrations provided the method parameters are known (pumping time, filter transfer time, count interval, system response) and these concentrations are constant during the pumping time. This is the inverse of the relation described in Appendix 5 which gives the number of each daughter decaying during the count interval and is not discussed in this report.

If the channel counts for channel T, B and X are \hat{T} , \hat{B} and \hat{X} and the number of decays of RaA, RaB and RaC/RaC' are A, B, C for the same interval then

$$\hat{T} = \epsilon_{\alpha} V_{T} (A+fC) + \epsilon_{\beta} V_{T} (B+C) + B_{T}$$
 (1)

$$\hat{B} = \epsilon_{R} V_{B} (B + C) + B_{B}$$
 (2)

$$\hat{X} = g \epsilon_{\alpha} V_{T} x \epsilon_{\beta} V_{B} x C$$
 (3)

where ϵ_{α} , ϵ_{β} are the α and β detection efficiencies $V_T,~V_R ~are~the~geometric~factors~associated~eith~T~and~B$

f = 1 - $e^{-\tau_C t}/\tau$ = 0.73 for τ = 180 μ s (dead time of T) and τ_{C^t} = 23.6 (mean life of RaC'); B_T , B_B are background counts of T and B; g = 1 - $e^{-G/\tau_C t}$ = 0.82 for gate G = 400 μ s.

Since \hat{X} is known, C can be calculated. Substitution of C into the second equation gives B; substitution of B + C and C into the first equation gives A.

This can be used to provide an estimate of the WL without any assumption as to the degree of equilibrium. However, the problem of statistical accuracy is inherent. This may be illustrated by the calculations below based on (i) 1 WL of radon daughters in secular equilibrium using an "ideal" system ($\varepsilon_{\alpha} = \varepsilon_{\beta} = 1$, $V_{T} = V_{B} = 0.5$, pump time 5 minutes at 10 1/m, transfer time 30s, count time 20 minutes, no background one would expect

Solving equations (1) to (3) give statistical errors from the counts

$$A = 4.2\%$$
 $B = 1.0\%$
C and C' = 0.7%

These figures may be obtained with the present system provided the geometric factors are optimised and the background kept low. (As mentioned, they are not the concentrations in air, but rather the total decays of each species on the filter paper, during the count interval.) (ii) only 0.01 WL, but otherwise identical conditions. The statistical errors in each estimate are

$$A = 37\%$$
 $B = 7\%$
 $C \text{ and } C' = 5\%$

The statistical error for the number of RaA decays, A has increased considerably, but the errors for RaB and RaC decays are acceptable.

The graph represents the percentage of each daughter decaying for a 5 minute sample time and a 30 second filter transfer time (from filter holder to the measuring system) for a variety of counting times. The lines A, B and C refer to an initial equilibrium mix of RaA, RaB and RaC in the air. The lines B* and C* are for "young" air when the initial concentration of RaA in air is 10 times that of RaB or RaC. The dashed lines are for background count rates of n, 2n, 3n,....and indicate that an optimization between counting time and background must be made.

The difference between C (secular equilibrium) and C* (0.1 equilibrium) in figure 32 for 20 minutes count time indicates that a measurement of WL based on RaC' alone could create an error $(C-C^*)$ of 25% in WL estimation if the degree of equilibrium was not known. This error could be reduced if the degree of equilibrium in the air is estimated. The high initial rate of decay from RaA $(T_{N_2}=3.05 \text{ min})$ demonstrated in figure 32 could be used in this respect.

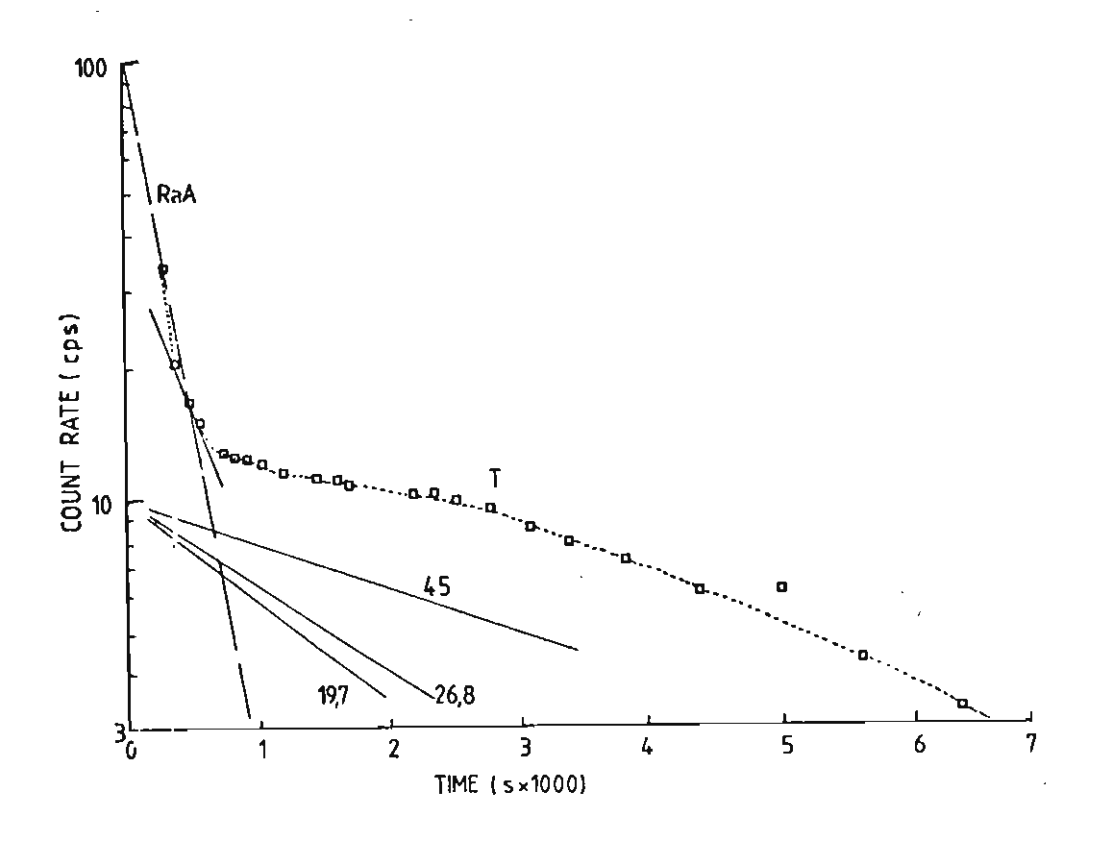


FIGURE 32 RUN 3 CHANNEL 'T' SHOWING THE HIGH INITIAL ACTIVITY OF RAA

5.6.7.2 Determination of WL by Measurement of Rac Alone

The last section (5.6.7.1) showed how all the short lived daughters of radon could be derived from the three channel counts. Consider the percentage contributions to one WL by the different daughters in secular equilibrium in table 1 (section 1.4).

RaA contributes 10% WL $(6.00 \text{MeV RaA}\alpha + 7.69 \text{ MeV RaC'}\alpha)$ RaB 53% WL $(\text{RaC'}\alpha)$ RaC/C' 38% WL $(\text{RaC'}\alpha)$

If only <u>total</u> RaC' is measured, then an estimation of the WL based only on RaC' would give the WL with an underestimate of only 4%. The figure below illustrates the problems associated with this approach.

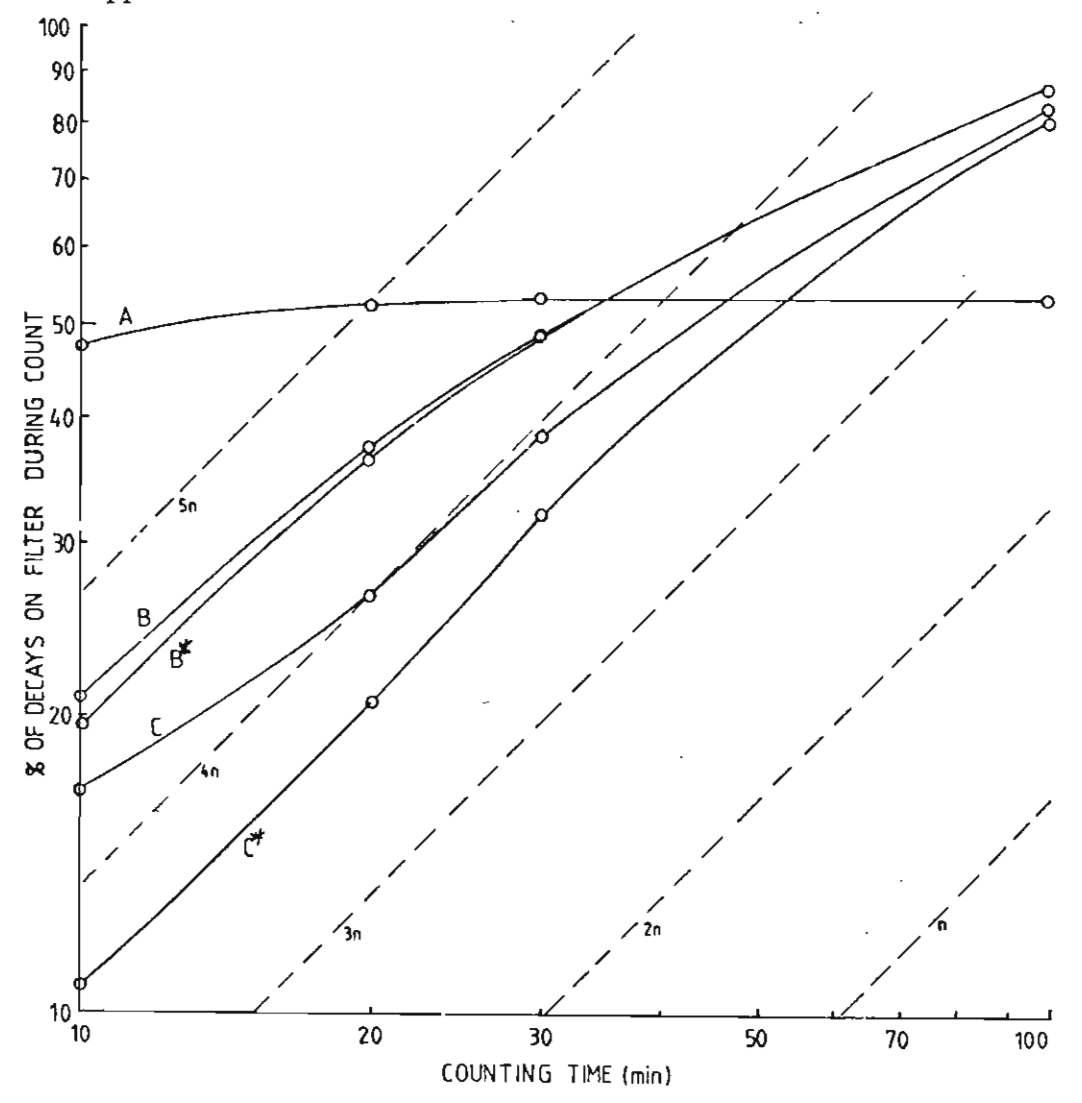


FIGURE 33 TOTAL DECAYS OF EACH DAUGHTER ON FILTER FOR
DIFFERENT COUNTING INTERVALS

A lack of knowledge about changes in the concentration of daughters during de-emanation prevented this analysis being performed, but the high equilibrium towards RaA is evident when the proportion of daughter activity from the RaA decaying on the filter is subtracted from the data at 2000s.

The main advantage of using just coincidence counts to estimate WL's is the degree of background rejection. This makes a direct WL estimate possible in the presence of other α emitters on the filters.

5.6.7.3 Determination of WL by RaB and RaC

The sensitivity of RaC to disequilibrium has been shown as the main problem of using only RaC as an indicator of WL for a limited (20 minute) count.

If the RaB decay is calculated from equation (2) in section 5.6.7.1 using data from channel 'B' and channel 'X' then a better estimation of WL can be made. Examination of figure 33 shows that RaB has a 3% sensitivity for a 20 minute count. A calculation from this data should give a total error of about 10% in estimating WL. This assumes the background count in channel 'B' is well known.

6. DISCUSSION

6.1 Summary of Results

The purpose of this study was

- (i) a laboratory investigation of delayed coincidence counting for RaC' determination.
- (ii) to investigate the application of this delayed coincidence count to WL estimates.

RaC' measurement by delayed coincidence counting was shown to be a reliable technique using cheap detectors and simple electronics. The background rejection in the coincidence channel at a relatively high count rate (16 cps) was over 30 in the presence of equal activity of 226 radium, 222 radon and RaA. An enironmental air sample collected on a filter would be unlikely to present such a high α background nor such a high count rate.

Two types of background can be present with filter methods. These are:-

- (i) that due to high activity in the environment e.g. γ rays, radon (and thoron). These may lead to direct counts on an instrument or a 'build up' of activity in the device. The GM detectors used in this study are relatively (1%) γ ray insensitive. In addition, adequate shielding and a background count can reduce this error.
- (ii) present in activity collected on the filter from long lived α emitters (^{238}U 4.18 MeV, ^{234}U 4.76 MeV, $^{210}\text{P}_0$ 5.298 MeV) in the air. To determine the background, a count must be taken hours after the radon daughter activity has decayed. An estimation of these factors is impossible from laboratory data but a reduction of background by a factor 30 has been shown and perhaps 100 can be expected in the coincidence channel. (At very low

count rates a reduction in background of several thousand could be expected with extended counts.)

The analysis in Section 5.6 shows that a variety of approaches can be applied to the estimation of the individual daughter concentrations. The result is to optimise either (i) the capability of the system to measure the degree of equilibrium with a low background or (ii) the ability to estimate a low WL in the presence of a high background. For the former, the intrinsic statistical errors were shown to be (for secular equilibrium)

	1 WL	0.01 WL
RaA decays	4.2%	` 37%
RaB decays	1.0%	7%
RaC decays	0.7%	5%

and for the latter ~25% for a measurement of RaC *alone*, in the absence of information about radioactive equilibrium in air. For a low WL, concentrating the activity by using a higher pumping rate would permit a better estimation of each total daughter decay.

6.2 Comparison With Other Methods

Other methods vary in the minimum activity detectable. Unfortunately, most of the data on the equipment is laboratory based and give little indication of the device performance in high backgrounds. A few different methods are tabulated below with the times necessary to perform the measurement.

	LOWER LIMIT OF DETECTION (WL)
BEDROSIAN (1969) Polaroid film/ ZnS (3h)	, 1
KUSNETZ (1969) filter/ZnS (45min)	0.3
ROLLE (1972) filter/ZnS (20min)	0.01
MARTZ (1969) surface barrier detector	0.01
CLIFF (1978) surface barrier detector for secular equilibrium	0.0001
NEW METHOD based on RaC' detection alone (20min)	0.0002

Although silicon surface barrier detectors show superior results, they are more expensive, require more complex electronics and are more fragile than the system proposed. Delayed coincidence considerably reduces the background and gives an isotope specific count, however, there is also a corresponding decrease in sensitivity, mainly due to the geometry and only counting one side of the filter. This is a necessary requirement when GM tubes are used since they have a long dead time. If a counter which could count α and β particles were used, with a small dead time, then only one detector need be used. This was demonstrated in the feasibility study with the gas flow proportional counter.

6.3 Improvements

The two main problems preventing thorough analysis of data were

- (1) A poor source of radon daughters. The radon jar was unsatisfactory for this study since the rate of de-emanation of any daughter activity was unknown. This made application and verification of the model developed difficult. A better source a large volume containing radon, would have produced more useful results.
- (2) A lack of knowledge about system performance.
- (i) The α and β detection efficiency of the GM tube used is considered "essentially 100%". This was not properly demonstrated.
- (ii) The uncertainties about determination of the various geometric factors from a purely theoretical view (Appendix 1) to the practical view, of what were the effective geometric distances.
- (iii) Complete lack of knowledge about the radial distribution of activity on the filter. It was assumed to be uniform for this study. A detector larger than the filter would eliminate

this problem. This error was expected to be small. Most of these three uncertainties could be overcome if a large thin α and β source were available. The time limit imposed on this study did not permit any of these problems to be completely examined.

CONCLUSION

A device capable of measuring environmental radon daughter activities in air has been demonstrated. A detection efficiency of 10% for RaA, B, C and 0.4% for RaC' for the prototype was calculated, although this could be improved at least fourfold by better selection of counting geometry. Isotope specific RaC' measurements were made in the presence of other α emitters in far greater concentrations. A lower limit of detection based on a 20 minute count of 10^{-3} WL based on RaC' detection was shown, but with better geometry a lower limit of detection of 2×10^{-4} could be achieved.

The device is the only non α spectroscopy method capable of providing definitive RaC/RaC' measurements and applicable to field use.

REFERENCES

- 1. AGOPSOWICZ, D.E. and NEWTON, G.J., 1979
 "A Real-Time Alpha-in-Air Monitoring System"
 Health Phys. 37: 379-382
- 2. ALTSHULER, B. and PASTERNACK, B., 1963
 "Statistical Measures of the Lower Limit of
 Detection of a Radioactivity Counter"
 Health Phys. 9: 293-298.
- 3. AUSTRALIAN GOVT. PUBLISHING SERVICE, 1975.
 "Code of Practice on Radiation Protection in the Mining and Milling of Radioactive Ores"
 Commonwealth Dept. of Health.
- 4. BAEDECKER, P.A., 1971 "Digital Methods of Photopeak Integration in Activation Analysis"
 Analytical Chemistry, 43, 3: 405-410.
- 5. BEDROSIAN, P.H., 1969 "Photographic Technique for Monitoring Radon-222 and Daughter Products" Health Phys. 16: 800-802.
- 6. BRAUER, F.P., KAYE, J.H. and CONNALLY, R.E., 1970 "X-Ray and β-γ Coincidence Spectrometry Applied to Radiochemical Analysis of Environmental Samples" in Advances in Chemistry Series, No. 93: 231.
- 7. BUDNITZ, R.J. 1974 "Radon-222 and It's Daughters -A Review of Instrumentation for Occupational and Environmental Monitoring" Health Phys. 26: 145-163.
- 8. CARCHON, R., et al, 1975 "A General Solid Angle Calculation by a Monte Carlo Method" Nuclear Instruments and Methods, 128: 195-199.
- 8. CHERRY, R.D., 1964 "Alpha Particle Detection Techniques Applicable to the Measurement of Samples from the Natural Radiation Environment" p407 of J.A.S. Adams and W. M. Lowder (Ed.)

 The Natural Radiation Environment, Univ. of Chicago Press, Chicago.
- 10. CLIFF, K.D. 1978, "The Measurement of Low Concentrations of Radon-222 Daughters in Air, with Emphasis on RaA Assessment" Phys. Med. Biol., 23,1: 55-65.

- 11. COCKETT, A.H. et al, 1975 "The Chemistry of The Monatomic Gases" from Pergamon Texts in Inorganic Chemistry Vol. 4, Pergamon Press, Oxford.
- 12. COMROE, J.H., 1966, "The Lung" p149 of Vertebrate Structures and Functions, Readings from Scientific American, W. H. Freeman and Co., San Francisco.
- 13. COOK, G.A., 1961, Argon, Helium and the Rare Gases Vol. 2.
- 14. CROSS, F.T., 1979, "Exposure Standards for Uranium Mining" Health Phys., 37: 765-772.
- 15. CROSS, P., and McBETH, G.W., 1976, "Liquid Scintillation Alpha Particle Assay with Energy and Pulse Shape Discrimination" Health Physics, 30 303-306.
- 16. DALU, G. and DALU, G.A., 1971, "An Automatic Counter for Direct Measurements of Radon Concentration" Aerosol Science, 2: 247-255.
- 17. DARRALL, K.G., RICHARDSON, P.J. and TYLER, J.F.C., 1973,
 "An Emanation Method for Determining Radium Using
 Liquid Scintillation Counting" Analyst, 98: 610-615.
- 18. DUGGAN, M.J. and HOWELL, D.M., 1969, "The Measurement of the Unattached Fraction of Airborne RaA" Health Phys., 17: 423-427.
- 19. ERLICK, A., et al, 1971, "Lifetime Measurements of Alpha Emitters in the Millisecond Region" Nuclear Instruments and Methods, 92 " 45-49.
- 20. EVANS, R.D., 1969, "Engineers' Guide to the Elementary Behaviours of Radon Daughters", Health Phys., 17: 229-252.
- 21. FIELDS, P.R., STEIN, L. and ZIRIN, M.H., 1963, "Radon Fluoride: Further Tracer Experiments with Radon" pl13 of H.H.

 Hyman (Ed), Noble-Gas Compounds, Univ. of Chicago
 Press, Chicago.
- 22. FRANK, A. L., and BENTON, E.V., 1977, "Radon Dosimetry Using Plastic Nuclear Track Detectors", Nuclear Track Detection, 1, 3/4: 149-179.

- 23. FREMLIN, J.H., 1964 "Measurement of Half-Life and Estimation of Rapidly Decaying Substances", pl47 of Applications of Nuclear Physics, The English Universities Press Ltd, London.
- 24. FRIEDLAND, S.S. and RATHBUN, L., 1980, "Radon Monitoring:

 Uranium Mill Field Experience with a Passive Detector"

 IEEE Transactions on Nuclear Science, NS-27,

 1: 704-712.
- 25. FRY, R.M., 1975, "Radiation Hazards in Uranium Mining and Milling" Atomic Energy, October 1975: 12-31.
- 26. GAMMAGE, R.B., KERR, G.D. and HUSKEY, L., 1976, "Exploratory Study of the Use of TSEE Dosimeters in Radon Monitoring", Health Phys., 30: 145-148.
- 27. GARDNER, R.P. and VERGHESE, K., 1971, "On the Solid Angle Subtended by a Circular Disc", Nuclear Instruments and Methods, 93: 163-167.
- 28. GEORGE, A.C. and HINCHLIFFE, L., 1972, "Measurements of Uncombined Radon Daughters in Uranium Mines" Health Phys., 23: 791-803.
- 29. GEORGE, A.C., 1972, "Measurement of the Uncombined Radon Daughters with Wire Screens", Health Phys., 23: 390-392.
- 30. GIFFIN, C., KAUFMAN, A., and BROECKER, W., 1963, "Delayed Coincidence Counter for the Assay of Actinon and Thoron", J. of Geophysical Research, 68, 6: 1749-1757.
- 31. GROËR, P.G., 1972, "The Accuracy and Precision of the Kusnetz Method for the Determination of the Working Level in Uranium Mines", Health Phys., 23: 106-109.
- 32. GUGGENHEIM, S.F. et al, 1979, "A Time-Integrating Environmental Radon Daughter Monitor:, Health Phys., 36: 452-455.
- 33. HARLEY, N.H., PASTERNACK, B.S., 1969, "The Rapid Estimation of Radon Daughter Working Levels When Daughter Equilibrium is Unknown", Health Phys., 17: 109-114.

- 34. HARSHAW, c1979, "Environmental Working Level Monitor", Company Brochure.
- 35. HOLADAY, D.A. et al, 1957, "Control of Radon and Daughters In Uranium Mines and Calculations on Biological Effects", U.S.P.H.S. Publication No. 494.
- 36. HOLMGREN, R.M. et al, 1977, "Relative Filter Efficiencies for Sampling Radon Daughters in Air", Health Phys., 32: 297-300.
- 37. HORROCKS, D.L., 1964, "Alpha Particle Energy Resolution in a Liquid Scintillator", The Review of Scientific Instruments, 35,3: 334-340.
- 38. JAFFEY, A.H., 1954, "Solid Angle Subtended by a Circular Aperture at Point and Spread Sources: Formulas and Some Tables", The Review of Scientific Instruments, 25, 4: 349-354.
- 39. JONASSEN, N. and McLAUGHLIN, J.P., 1976, "The Effect of RaB Recoil Losses on Radon Daughter Measurements" Health Phys., 30: 234-238.
- 40. KIEFER, H. and MAUSHART, R., 1972, Radiation Protection Measurement, p264. Pergamon Press, Oxford.
- 41. KUSNETZ, H.L., 1956, "Radon Daughters in Mine Atmospheres", American Industrial Hygeine Assoc. Quarterly, 17.
- 42. LAWRENCE, J.H., et al, 1946, "Preliminary Observations on the Narcotic Effect of Xenon with a Review of Values for Solubilities of Gases in Water and Oils", J. Physiol., 105: 197-204.
- 43. LEDERER, C.M., 1978, Table of Isotopes.
- 44. LINDEKEN, C.L. et al, 1964, "Surface Collection Efficiency of Large-Pore Membrane Filters", Health Phys., 10: 495-499.
- 45. LUCAS, H.F., 1957, "Improved Low-Level Alpha-Scintillation Counter for Radon" The Review of Scientific Instruments, 28, 9: 680-683.
- 46. McCURDY, D.E., SCHIAGER, K.J. and FLACK, E.D., 1969, "Thermoluminescent Dosimetry for Personal Monitoring of Uranium Miners", Health Phys., 17: 415-422.

- 47. McDOWELL, W.J., 1975, "High-Resolution Liquid Scintillation Method for the Analytical Determination of Alphs-Emitters in Environmental Samples", IEEE Transactions on Nuclear Science, NS-22; 649-653.
- 48. MALLER, R.A., 1979, "On the Precision of Estimation of Half Life In Delayed Coincidence Experiments"

 Nuclear Instruments and Methods, 167: 479-481.
- 49. MARTZ, D.E., et al, 1969, "Analysis of Atmospheric Concentrations of RaA, RaB and RaC by Alpha Spectroscopy", Health Phys., 17: 131-138.
- 50. MERCER, T.T., 1976, "The Effect of Particle Size on the Escape of Recoiling RaB Atoms from Particulate Surfaces", Health Phys., 31: 173-175.
- 51. MOODY, G.J. and THOMAS, J.D.R., 1964; Noble Gases and Their Compounds, Pergamon Press, Oxford.
- 52. NEWSTEIN, H., COHEN, L.D. and KRABLIN, R., 1971, "An Automated Atmospheric Radon Sampling System", Atmospheric Environment, 5: 823-831.
- 53. PALTRIDGE, G.W., 1967, "The Retention of Atmospheric Radioactivity by Fibrous Filters", J. of Geophysical Research, 72, 4: 1269-1273.
- 54. PERDUE, P.T., DICKSON, H.W. and HAYWOOD, F.F., 1980, "Radon Monitoring Instrumentation", Health Phys., 39: 85-88.
- 55. PRICHARD, H.M. and GESSELL, T.F., "Rapid Measurements of 222 Rn Concentrations in Water with a Commercial Liquid Scintillation Counter", Health Phys., 33: 577-581.1977.
- 56. RAABE, O.G., 1968, "Measurement of the Diffusion Coefficient of Radium A", Nature 217: 1143-1145.
- 57. RAABE, O.G., 1969, "Concerning the Interactions That Occur Between Radon Decay Products and Aerosols", Health Physics, 17: 177-185.
- 58. RANDOLPH, H.W., 1971, "Sampling by Laminar Flow Entrainment to Prevent Wall Effects" Nuclear Instruments and Methods 92: 233-235.

- 59. ROBERTS, P.B. and DAVIES, B.L., 1966, "A Transistorized Radon Measuring Equipment", J. Sci. Instrum., 43: 32-35.
- 60. ROLLE, R., 1969, "Improved Radon Daughter Monitoring Procedure", Amer. Indust. Hygiene Assoc. Journal, Mar-Apr, 1969: 153-160.
- 61. RUBY, L., and RECHEN, J.B., 1968, "A Simpler Approach to the Geometrical Efficiency of a Parallel-Disc Source and Detector System", Nuclear Instruments and Methods, 58: 345-346.
- 62. SCHERY, S.D., GAEDDERT, D.H. and WILKENING, M.H., 1980, "Two-Filter Monitor for Atmospheric 222Rn", Rev. Sci. Instrum, 51, 3: 338-343.
- 63. SCHULZE, A., 1920, "Über die Löslichkeit der Radiumemanation in Organischen Flüssigkeiten", Z. physik chemie, 95: 257-279.
- 64. SPARROW, E.M. and CESS, R.D., 1978, Radiation Heat Transfer, McGraw-Hill Book Co., New York.
- 65. SPIEGAL, M.R., 1975, Probability and Statistics, McGraw-Hill Book Co., New York.
- 66. STEIN, L., 1970, "Ionic Radon Solutions", Science, 168: 362-364.
- 67. STEIN, L., 1973, "Removal of Xenon and Radon from Contaminated Atmospheres with Dioxygenyl Hexafluoroantimonate, 0₂SbF₆",

 Nature, 243: 30-31.
- 68. STEIN, L., 1974, "Noble Gas Compounds: New Methods for Collecting Radon and Xenon", Chemistry, 47, 9: 15-20.
- 69. THOMAS, J.W., and Le CLARE, P.C., 1970, "A Study of the Two-Filter Method for Radon-222", Health Phys., 18: 113-122.
- 70. TREMBLAY, R.J. et al, 1979, "Measurement of Radon Progeny Concentration in Air by α -Particle Spectrometric Counting During and After Air Sampling", Health Phys., 36: 401-411.

- 71. TSIVOGLOU, E.C., AYER, H.E., and HOLADAY, D.A., 1953, "Occurrence of Nonequilibrium Atmospheric Mixtures of Radon and its Daughters", Nucleonics 11, 9: 40-45.
- 72. WILLIAMS, I.R., 1966, "Monte Carlo Calculation of Sourceto-Detector Geometry", Nuclear Instruments and Methods 44: 160-162.
- 73. YANG, F., and TANG, C., 1978, "A General Formula for the Measurement of Concentrations of Radon and Thoron Daughters in Air", Health Physics, 34: 501-503.

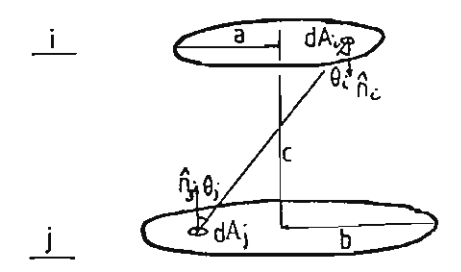
APPENDIX 1

GEOMETRIC FACTOR

The conventional approach to determining the geometric factor of a coaxial disc source/detector geometry is to use the solid angle subtended by a point to a detector and integrate it over the source. This gives an integral which cannot be solved exactly but at a distance can be approximated by a polynomial (JAFFEY, 1954). A Monte Carlo approach(CARCHON, 1975) may also be taken, or the integral may be expressed in terms of Bessel functions or Legendre polynomial (WILLIAMS 1966, RUBY, 1968). This approach appears in error since a point source is a volume element and when integrated over a disc must produce a volume integral.

A different approach is to consider a surface element of the source and a surface element of the detector (SPARROW 1978) and to perform the double integral.

Comparing the integrals for the two approaches, shows the formulation for the geometric factor V_{i-j} to be similar.



JAFFEY →

$$\pi^2 \frac{b^2}{c} V_{A_i - A_j} = \int_{A_i A_j} \frac{dA_i dA_j}{r^3}$$

$$= \int_{0}^{2\pi} d\theta_{i} \int_{0}^{b} r_{i} dr_{i} \int_{0}^{2\pi} d\theta_{j} \int_{0}^{a} \frac{r_{j} dr_{j}}{[r_{i}^{2} + r_{j}^{2} - 2r_{i} r_{j} \cos(\theta_{i} - \theta_{j}) + c^{2}]^{3/2}}$$

whereas SPARROW →

$$\pi^{2} \frac{b^{2}}{c^{2}} V_{A_{i}-A_{j}} = \int_{A_{i}-A_{j}} \frac{dA_{i}dA_{j}}{r^{4}}$$

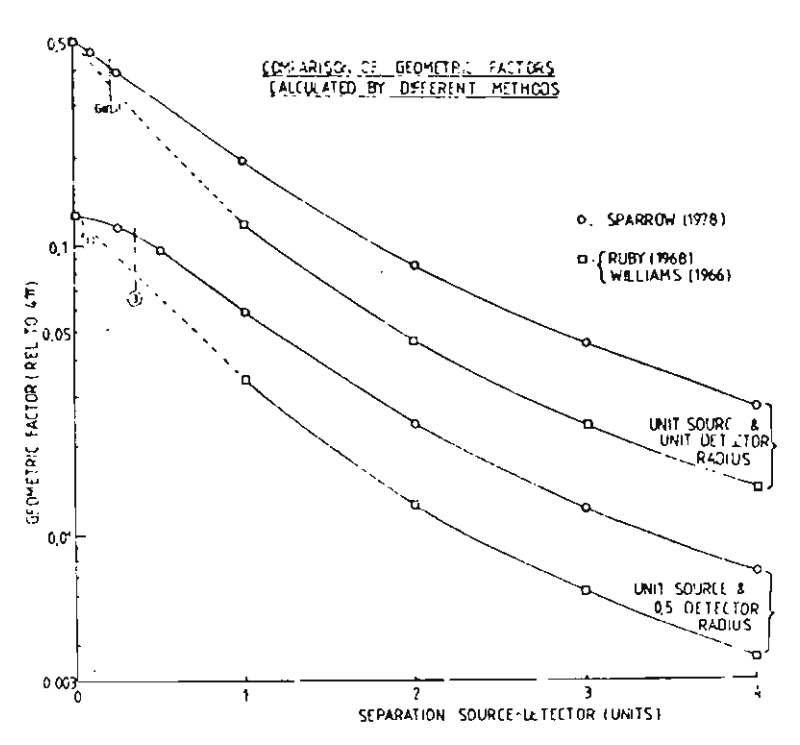
$$= \int_{0}^{2\pi} d\theta_{i} \int_{0}^{b} r_{i}dr_{i} \int_{0}^{2\pi} d\theta_{j} \int_{0}^{a} \frac{r_{j}dr_{j}}{[r_{i}^{2}+r_{j}^{2}-2r_{i} r_{j} \cos(\theta_{i}-\theta_{j}) + c^{2}]^{2}}$$

$$\rightarrow V_{S-D} = \frac{1}{2} (Z - \sqrt{Z^{2} - 4X^{2}Y^{2}})$$
where $X = a/c$, $Y = c/b$,
$$Z = 1 + (1 + X^{2}) Y^{2}$$

A short program was written to calculate this factor.

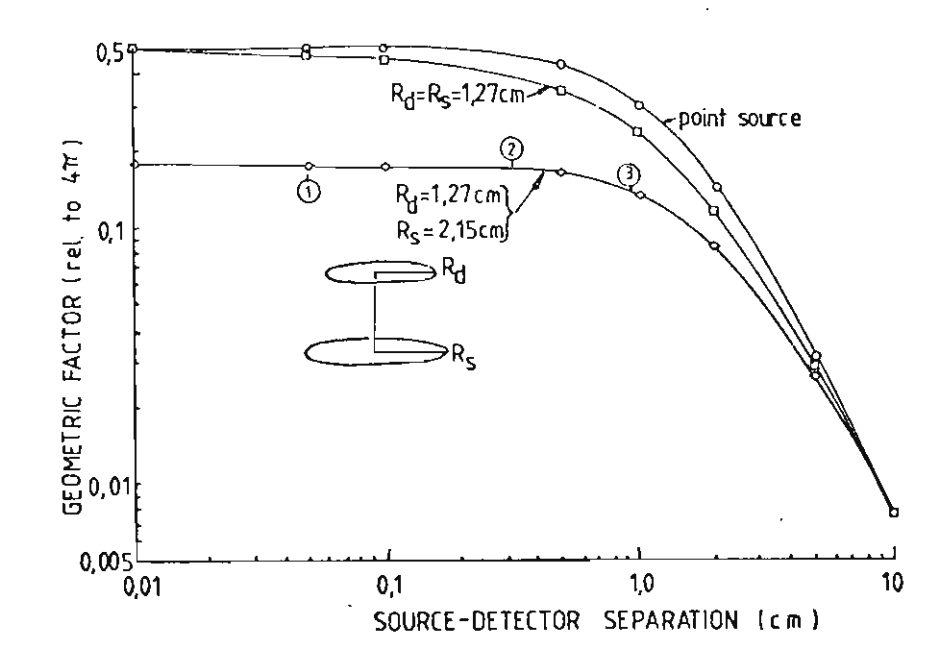
When the separation c is zero or infinite the solutions are the same. (At C=0,V is the ratio of the detector to source area, at large distances the source is similar to a point source).

The graph below illustrates the difference between the approaches. The lower plots show the geometry used for this study.



The appraoch by SPARROW shows a shoulder at small distances apparently not predicted by the approach of RUBY or the "Monte Carlo" method of WILLIAMS. This would be expected, especially for small detectors, when the source approximates to an infinite plane at small separations.

The second graph (below) shows the geometric factor calculated using SPARROW's method for the system. (Points 1, 2 and 3 are the geometric factors for the bottom channel B (1); the top channel T in Run 1 and Run 2 (2); Run 3 (3).

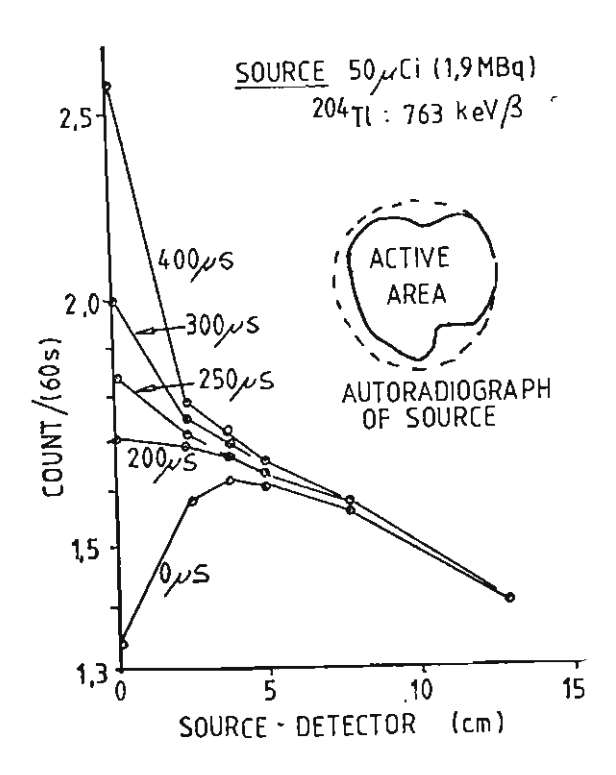


GEOMETRIC FACTOR BY SPARROW'S METHOD

Empirical tests of the new relationship were tried, but a large uniform thin source was not available. The diagram below shows (i) an autoradiograph of the best distributed β source available and (ii) a plot of a geometry corrected count at various distances for various dead times. A distributed α source was not available.

The plots for different dead times were made because of statistical uncertainties in the dead time calculations for this experiment. A plot using the correct dead time would give a horizontal line if the geometric factors were correct.

Nothing conclusive may be said from this study since (i) effective source/detector distance was not known; (ii) the source was not uniform.



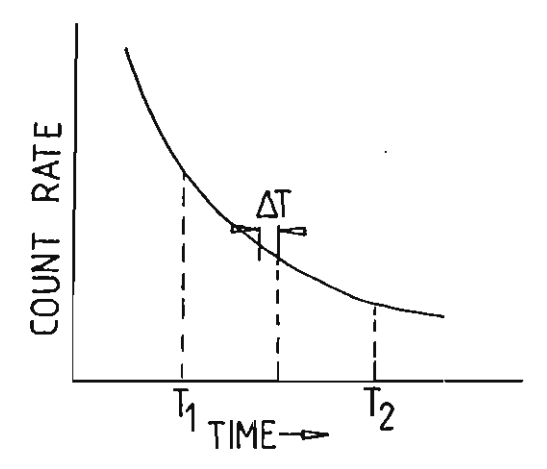
CHANGE IN DISTANCE-CORRECTED (SPARROW)
COUNT FOR VARIOUS SYSTEM CHANNEL DEAD TIMES

RAPID DECAY CORRECTION

For a single isotope decaying at a rate comparable to the measuring interval, the mean sampling time will over-estimate the average count rate. This is because more decays occur in the first half than the second half of the interval.

FREMLIN (1964) shows a simple correction to the mean count time to correct this error. For a measuring interval $t_1^{\rightarrow}t_2$, the correction is

$$\Delta t = 1.443 \, T_{\chi} \ln \left[\sinh(0.347(t_2 - t_1) / T_{\chi}) \right] / \left[0.347(t_2 - t_1) / T_{\chi} \right]$$



A short program was written to evaluate Δt for RaA, RaB or RaC for different counting times. For example,

daughter	count time (s)	correction (s)
RaA	100	1.6
RaB	600	6.4
RaC	600	8.8

The correction was not applied to the graphing of the results, since the correction was small, could be positive or negative (buildup or decay) and complex, since a correction weighted for each daughter activity would have to be used. Also, the RaA activity was negligible after the first 20 minutes.

PROPERTIES OF RADON

There is relatively little information on the physical and chemical properties of radon. This appendix summarises some of the more useful properties.

CHEMICAL

STEIN (1970) demonstrated the formation of stable radon fluoride from halide fluorides at room temperature, and suggests its use for collection of radon. This may be a viable technique for sampling, but as EVANS (1969) points out "heroic radiation gamma ray shielding" would be required on a chemical scrubber.

STEIN (1974) has reviewed a number of new antimony and bismuth compounds based on halide fluorides. They react with radon and produce oxygen, e.g.

$$R_n + 20_2^+ SbF_6^- \rightarrow R_n F^+ Sb_2 F_{11}^- + 20_2$$

(Similar reactions are suggested to capture xenon which are applicable to safe disposal of 133 and 127 xenon in hospitals).

WEINSTOCK (footnote in FIELDS 1963) suggests the formation of a stable radon silicate in a quartz microwave discharge.

BARTLET (in COCKETT 1975) reviews some work including STEIN (1970) and postulates more complex salts of radon. Clathrates of all the noble gas with the general formula 8G.46H₂O have been known for many years. Clathrates of radon with hydrogen chloride, bromide and sulphide have been used to separate radon from helium and neon.

COCKETT (1975) states "radon is strongly absorbed on solid radium surfaces".

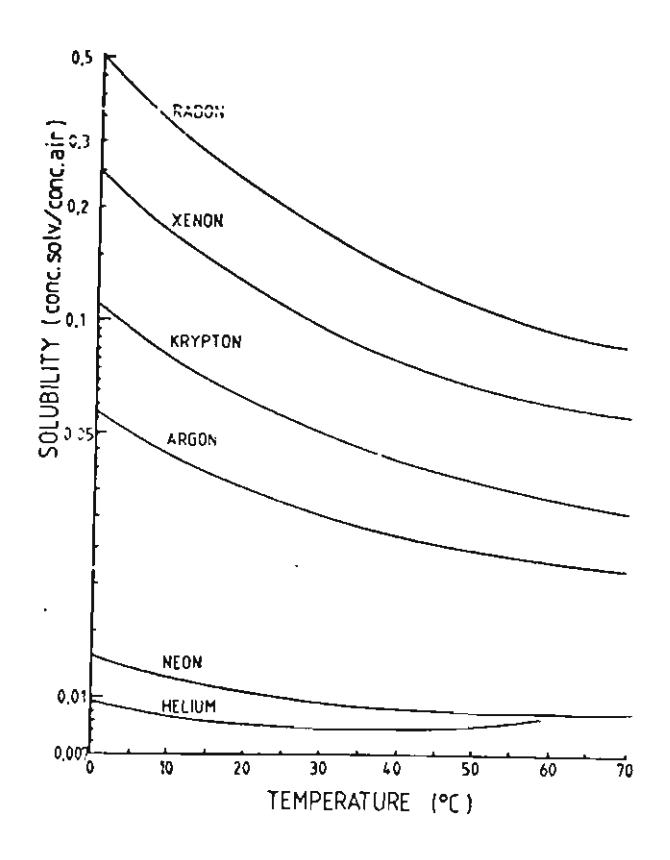
PHYSICAL

Two books (COOK 1961, COCKETT 1975) contain tables of physical properties, though it is more likely that the chemical properties, including solubility are of more use at very low concentrations.

The solubility of radon in various fluids was studied many years ago (SCHULZE 1920). The solubility of a gas may be defined as the ratio of its concentrations above and in the solvent. The following tables and graphs show the solubility of radon in various fluids, and may provide the basis for a sampling technique.

The solubility of radon in water is greater than that of the other inert gases (LAWRENCE 1946).

SOLUBILITY IN WATER



The solubility of radon in water has been examined by SCHULZE (1920) the table and graph below shows this.

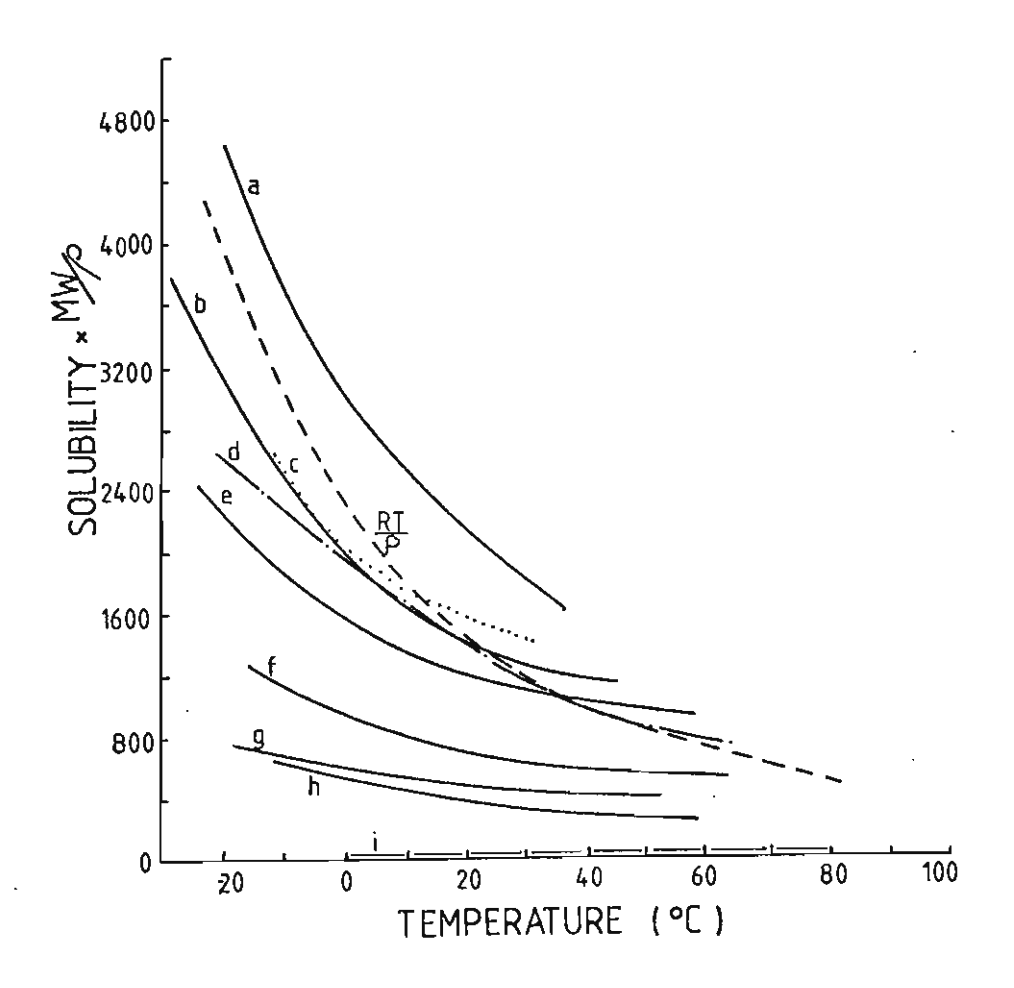
Results of Schulze, 1920

The results are given in terms of the Ostwald solubility expression ℓ , which is the relation of the concentration of the gas in the liquid to that in the gas space.

Solubility of Radium Emanations, & in:

t°	Toluene	Ether	CHC13	Acetone	೧೮₂	CH3COOC2H5	C2H5OH	Hexane
	ď	د	e	9	ь	£	h	a
- 18	27.0	29.1	28.4	10.7	50.3	13.6	11.4	35.2
- 10	22.5	-	23.8	9.3	41.5	_	-	28.5
- 5	20.6	21.9	21.6	8.5	37.0	_	•	25.7
0	18.4	19.9	19.6	8.0	33.4	9.41	8.28	23.4
÷ 5	17.0	18.2	18.1	7.4	-	-	_	21.4
10	15.7	16.9	16.7	6.9	27.2	8.0	6.93	19.6
15	13.9	15.8	15.6	6.5	_	-	-	17.9
18	13.2	15.1	15.0	6.3	23.1	7.16	6.17	16.6
20	_	14.8	14.6	6.1	-	_	6.03	-
25	11.4	14.0	13.8	5.8	21.5	6.57	_	14.7
30	10.5	13.3	13.1	5.6	20.1	-	5.30	13.3
40	8.87	-	11.9	5.2	18.1	5.64	4.72	-
50	7.6	-	11.2	-	-	5.22	4.26	-
60	6.42	-	-	-	-	4.9	-	~

The solubility in aniline is 4.43 at 0° and 3.8 at 18°.
The solubility in benzene is 12.82 at 18°.
The author also quotes data for the densities of the solvents at the several temperatures.



TWO FILTER TUBE AND PLANCHET

I TWO FILTER TUBE - DESIGN CONSIDERATIONS

It was intended to not only sample the radon daughters, but to measure the radon concentration. A two filter tube was built after the design in a review paper by THOMAS and LeCLARE (1970). A simplified design evolved, with a good aerodynamic design and high (92%) utilization of the filter area. This compares with 52% utilization for a commercial filter air sampler (ELECTRONIC FLOW METERS LTD, HOUNSLOW, ENGLAND). This is important at high flow rates since it reduces the linear air velocity, the limiting factor with membrane filters. If a portable pump is used, a lower resistance to flow for a given flow rate would be found.

THOMAS and LeCLARE found that a diffusion coefficient of 0.085 cm²/s (c.f. 0.050 cm²/s RAABE 1968) was needed for RaA (This may be partly due to unsteady laminar flow through the tube due to aerodynamic roughness imposed on the flow by the tube entrance.)

Examination of the attached working drawings show very little interference with any flow stream lines. An excellent seal was demonstrated between the filters and the '0' rings when left overnight. A thin ring of filter paper broke away when the '0' ring was removed from the filter. Only gentle forces are needed to assemble and disassemble the system. The small contact area between '0' ring and filter produced very high sealing pressures. The absence of a screw action made machining of the assembly easier and meant that a washer was eliminated from the design.

BACKING GAUZE

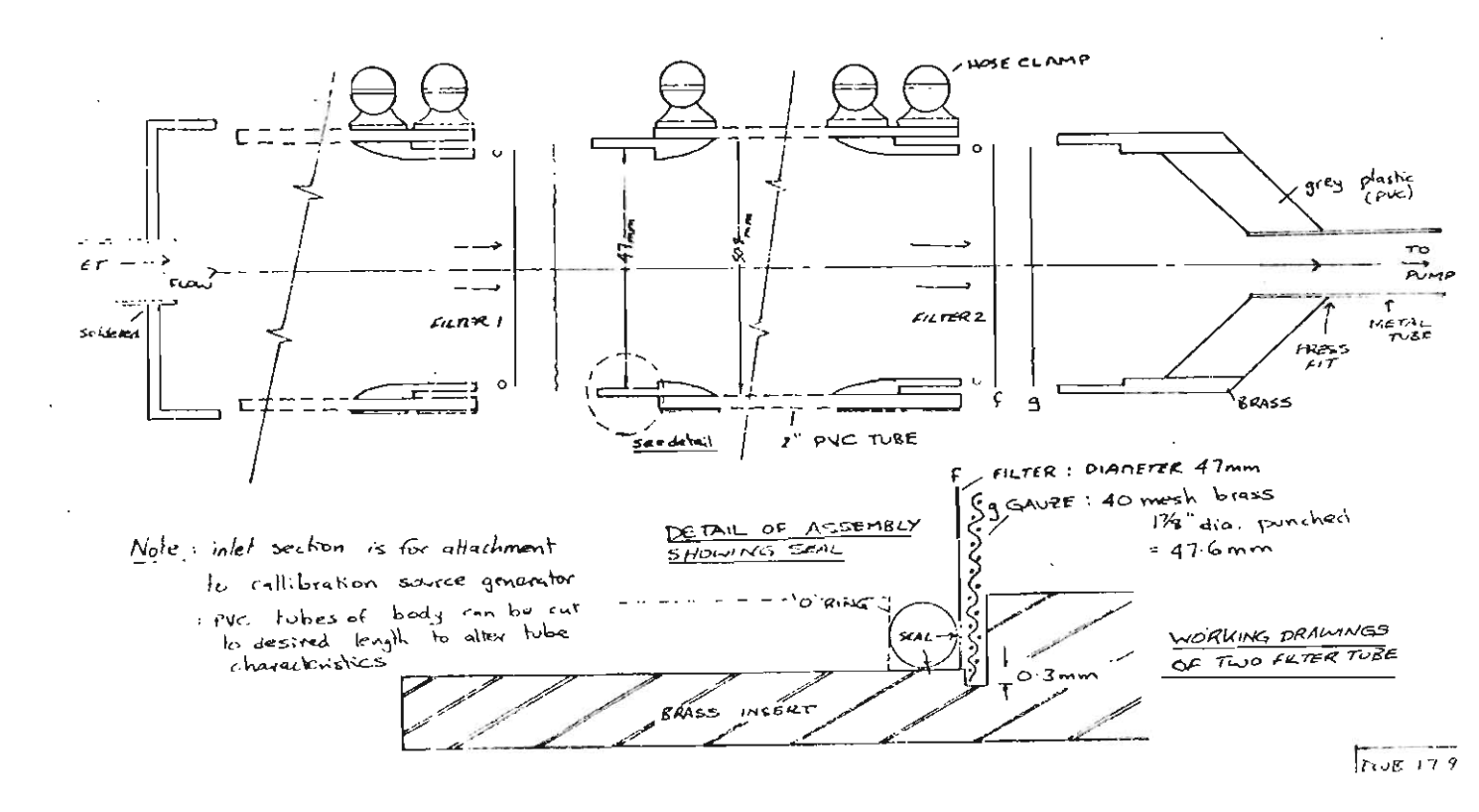
The backing gauze to hold the filter was punched from a sheet of gauze (40 mesh brass of 0.010 "thou" wire). A finer mesh (60 mesh) was tried but lacked rigidity when used at a high pump rate, but coarser gauze, when reinforced with paper clip "crosshairs" spot soldered lightly to the back, gave sufficient rigidity. The mesh clipped securely into a 0.3mm angular groove.

The assembly was pressurized to 200 kPa (30 psi) and when submerged the absence of bubbles indicated air-tightness.

A half turn on the hose clamps locking the assembly together quickly released the assembly for removal of the filter. The design of the system meant that only one '0' ring per section was needed.

Should a different length decay tube between the filters be needed, it is a simple and cheap operation to cut another section of plastic tube.

Only the first stage of the filter tube - to collect radon daughters, was used in this study.

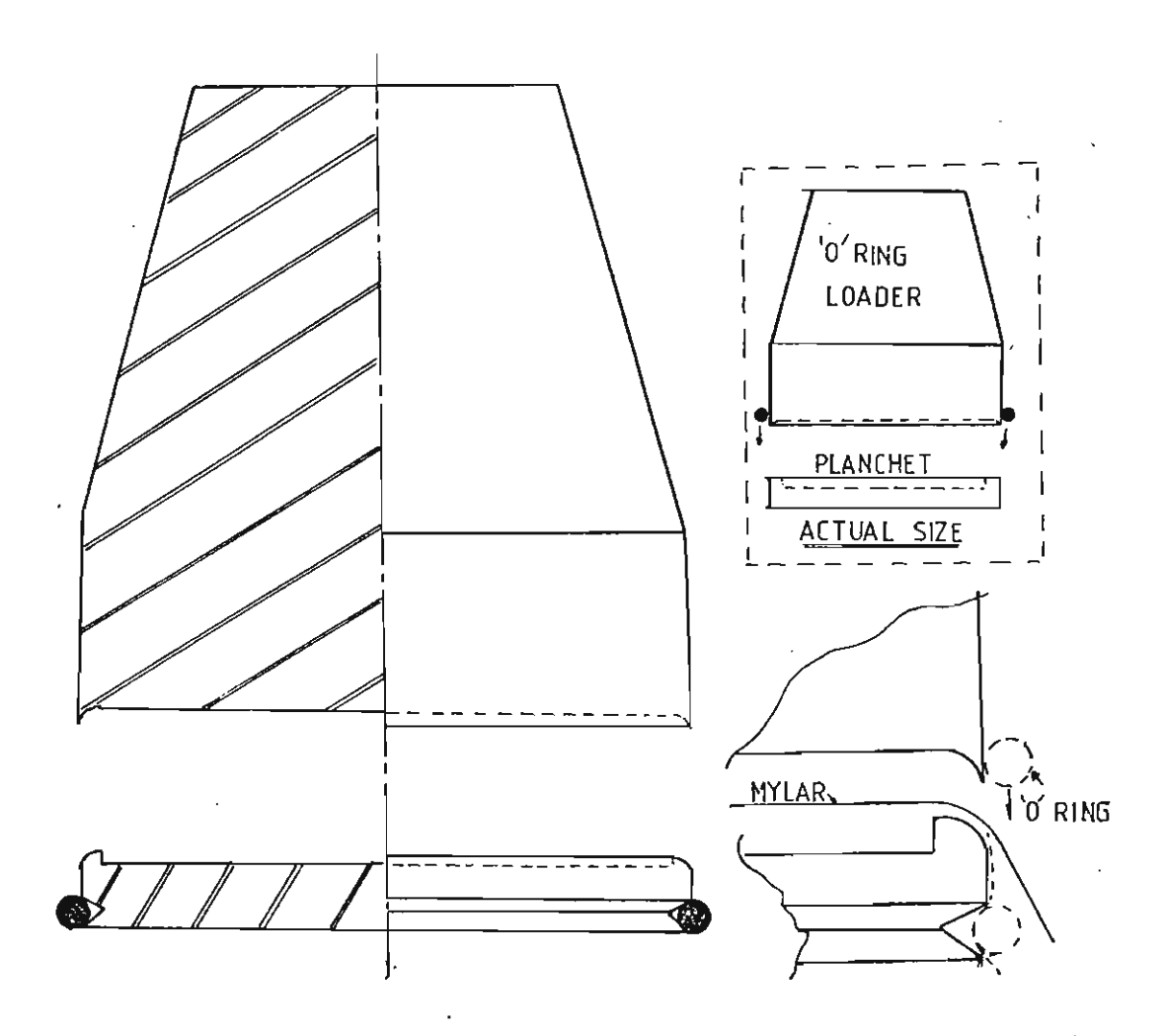


II PLANCHET DESIGN

A small planchet to fit the gas flow proportional counter (EBERLINE model FC 1) was constructed. The device was designed to make a gas tight container with a thin window in lieu of a thin window on the proportional counter, to reduce the flushing time of the counter and to allow a build up of radon gas within it.

The aim of this was to produce a calibration source of radon daughters.

The figure below illustrates the design of the planchet and '0' ring loader. The sample is placed in the depression in the planchet and sealed by a thin film of mylar, held in place by the '0' ring.



MODEL OF SYSTEM

YANG (1978) gives a generalised formula for calculating the numbers of each daughter nuclei decaying during a counting interval $T_1 \rightarrow T_2$ after sampling for time t_0 for the decay RaA \rightarrow RaB \rightarrow RaC.

$$\begin{split} N_{A}(\tau_{0}; T_{1} \rightarrow T_{2}) &= 2.22 \epsilon F Q \tau_{A}^{2} f_{A}^{C} C_{A}, \\ N_{B}(\tau_{0}; T_{1} \rightarrow T_{2}) &= 2.22 \epsilon F Q \left\{ \left(\frac{\tau_{A}^{3}}{\tau_{A}^{-\tau_{B}}} f_{A} \right) C_{A} + \tau_{B}^{2} f_{B}^{C} C_{B} \right\} \\ &+ \frac{\tau_{B}^{2} \tau_{A}}{\tau_{B}^{-\tau_{A}}} f_{B} C_{A} + \tau_{B}^{2} f_{B}^{C} C_{B} \\ N_{C}(\tau_{0}; T_{1} \rightarrow T_{2}) &= 2.22 \epsilon F Q \left\{ \left(\frac{\tau_{A}^{4}}{(\tau_{A}^{-\tau_{B}})(\tau_{A}^{-\tau_{C}})} f_{A} \right) + \frac{\tau_{B}^{3} \tau_{A}}{(\tau_{B}^{-\tau_{A}})(\tau_{B}^{-\tau_{C}})} f_{B} \right\} \\ &+ \frac{\tau_{C}^{3} \tau_{A}}{(\tau_{C}^{-\tau_{A}})(\tau_{C}^{-\tau_{B}})} f_{C} C_{A} \\ &+ \left(\frac{\tau_{B}^{3}}{\tau_{B}^{-\tau_{C}}} f_{B} + \frac{\tau_{C}^{2} \tau_{B}}{\tau_{C}^{-\tau_{B}}} f_{C} \right) C_{B} \\ &+ \tau_{C}^{2} f_{C} C_{C} \right\} \end{split}$$

where
$$f_{i} = (1-e^{-t}0/\tau_{i})(e^{-\tau/\tau_{i}}-e^{-\tau_{i}})$$
 i=A, B, C (2)

 τ_A , τ_B and τ_C are the mean lifetimes (in minutes) of RaA, RaB, RaC; ϵ is the counter efficiency referred to 4π ; F is the filter coefficient including self absorption; C_A , C_B ,

 C_{C} are the concentrations in air of RaA, RaB and RaC in pCi/l; $Q = pump \ rate \ 1/min$.

A modified form of this model (F = 1, ϵ = 1) was used to predict counts expected in channels T, B and X in the system.

CHANNEL B

The detection efficiency (ϵ_{β}) of β particles in the energy range 0.72 (RaB)+3.17 (RaC) MeV was assumed the same (~100%). For a Geometric (or View) factor V_B for the bottom channel the number of counts will be

$$B = \epsilon_{\beta} V_{B} (N_{B} + N_{C}) + B_{b}$$

where B_b is the background count. The dead time may be ignored at low count rates (10 cps).

CHANNEL T

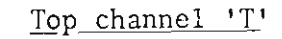
The predicted count is more complicated for the top channel since both α and β particles are detected. The α detection efficiency ϵ_{α} was assumed the same for the 6.00 (RaA) α and 7.68 (RaC') α particles (again ~100%). Since RaC' has a short half life (164 μ s) the channel dead time becomes significant.

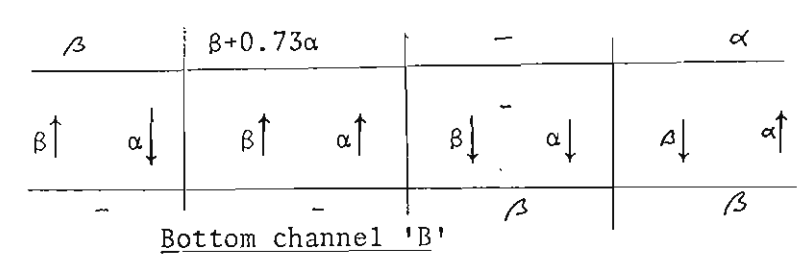
If A RaC β is detected by channel T, then only RaC' α 's decaying after the channel is ready again, will be detected. The proportion is

1 -
$$e^{-\tau}C^{1/\tau}$$

where τ_{C} is the mean life (236.6µs) of RaC and τ is the top channel dead time (inµs).

For the stated channel dead time (400 μ s) the fraction is 44.6% but for the measured channel dead time (~180 μ s) the fraction would be 73.1%. The total fraction of RaC' α 's detected by 'T' is





 $\frac{1}{2} \times (0.73 + 1) = 0.86$ of those α 's directed upwards. The counts in channel 'T' will be

$$\hat{T} + V_T[\epsilon_{\alpha} (N_A + 0.86 N_{C-} + \epsilon_{\beta}(N_B + N_C)] + B_t$$

at low count rates. Note that $N_C = N_C$, and the geometric factor V_{τ} (referred to 4π) compensates for the lack of detection downwards.

COINCIDENCE CHANNEL 'X'

The number of coincidence counts depends on the number of RaC β 's detected in channel 'B' followed by a RaC' detected by channel T, i.e.

$$\hat{X} = V_T \epsilon_{\alpha} \times V_B \epsilon_{\beta} \times N_C$$

The coincidence 'background' is count rate, which changes during the count period. The random coincidence background count rate \hat{X}_R is given by

$$X = (V_T[\varepsilon_{\alpha}(\mathring{N}_A + .86N_C) + \varepsilon_{\beta}(N_B + N_C)] + B_T)_{x}$$
$$(V_B[\varepsilon_{\beta} \mathring{N}_B] + B_B) \times G$$

For a 400 μ s gate, G = 6.7 x 10⁻⁶ min. The random coincidence background count rate is overestimated by

 \mathring{X} = \mathring{T} \mathring{B} G and the total random coincidence background can be underestimated by up to a factor of 2 or 3 by

$$x_{B} = \frac{\ddot{T} \ddot{B} G}{T_{2} - T_{1}}$$

A good estimate of $\boldsymbol{X}_{\boldsymbol{B}}$ requires a piecewise integration of

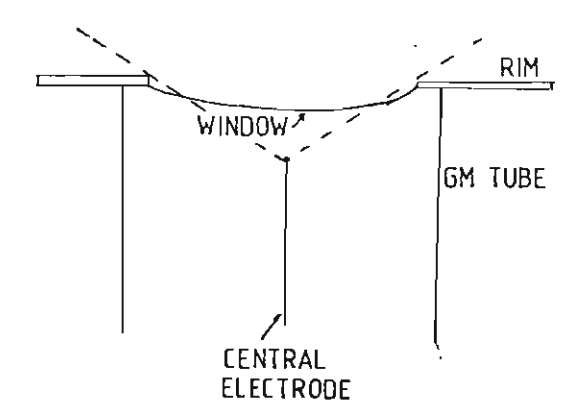
$$\overset{\circ}{X}_{B}$$
 over $T_{1} \xrightarrow{} T_{2}$.

An attempt to fit the model to Run 3 was attempted but the lack of knowledge of the effective values for a number of parameters made a partial fit only possible. A program was written to calculate $N_{\mbox{A}}$, $N_{\mbox{B}}$, $N_{\mbox{C}}$ and T, B, X. The difficulties were:-

1. Geometry

The effective source detector distance is not the physical distance since

- (a) The detector sensitive volume lies behind the window. Also, the window is slightly curved.
- (b) The detector does not have a 2π sensitivity since there is a rim on the cap holding the detector.



2. Efficiency

The detection efficiency is going to depend to some extent on the angle of incidence of the particle. This is going to be more important for α than β particles since α particles have a more limited range. The use of membrane filters ensures the activity is very much on the surface of the filter. An estimate of filter penetration of small (<1 μ) particles from electron microscopy (Appendix 7) is about 1μ so "burial losses" should be little problem.

RaC¹

The detection efficiency of RaC', especially near the end of the count when the activity of RaC' ~ RaB is important. This is strongly dependent on the channel dead time. Most of these difficulties could be overcome by the construction of a thin source of the same size as the filter, and using a filter the same diameter or smaller than the detector. This would overcome problems relating to ununiform deposition of activity (greater in centre) on the filter during sampling.

4. Sampling

concentration during sampling. This was especially so in this study, where the sampling period was 5 minutes, but the effective time would have been closer to 30s. A better method of generating radon daughters would be to de-emanate the radon jar into a weather balloon through a filter and wait for the required degree of equilibrium between radon and newly formed radon daughters before sucking the mix through the filter.

Various radon concentrations could be made by partially filling the balloon with radon and then topping it up with air.

5. Background

A factor of 10 increase in background in the top channel was measured during a run. This may be due to the radon levels in the laboratory increasing (the fume cupboard extractor fans were weak) from de-emanated radon. This is reflected in the asymptotic behaviour of all channel hours after the run to a background for higher than the pre-run background, even with the filter removed.

The upper GM tube background was reduced by 'cleaning' it and removing the stagnant air surrounding it with compressed air, during a test but not during a 'run'.

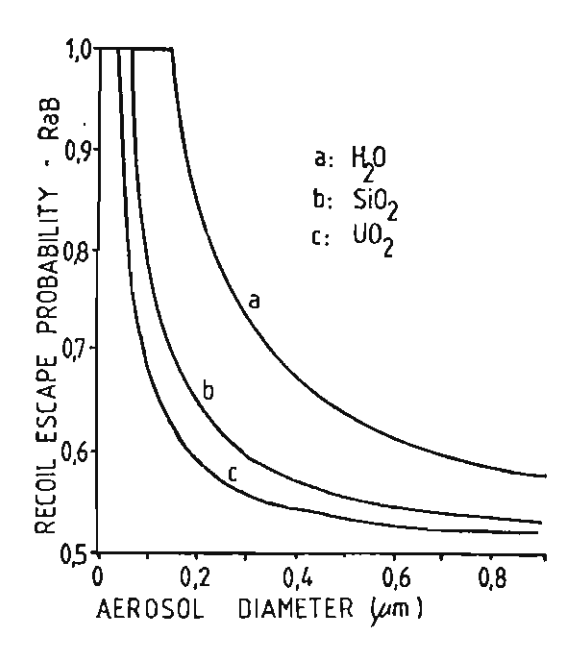
A permanent reduction in some of this background would be achieved by sealing the detector body from the air.

RECOIL LOSSES

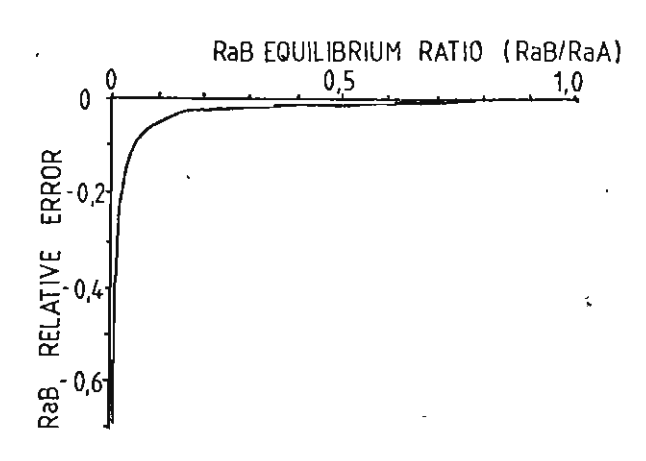
RaB

The recoil energy from α emission following RaA decay is taken up by the RaB nucleus. Since the binding energy to an aerosol particle is about one electron volt, there is a good chance of detachment of an attached daughter. Since the RaB nucleus could escape by tunnelling out of or through a particle, the size and stopping power of the particle is important. This will depend on the range of the RaB nucleus in the particle. MERCER (1976) tabulates ranges and graphs the probabilities.

	Air	H ₂ 0	Si0 ₂	U0 ₂
RaB range (µm)	120	0.13	0.057	0.035

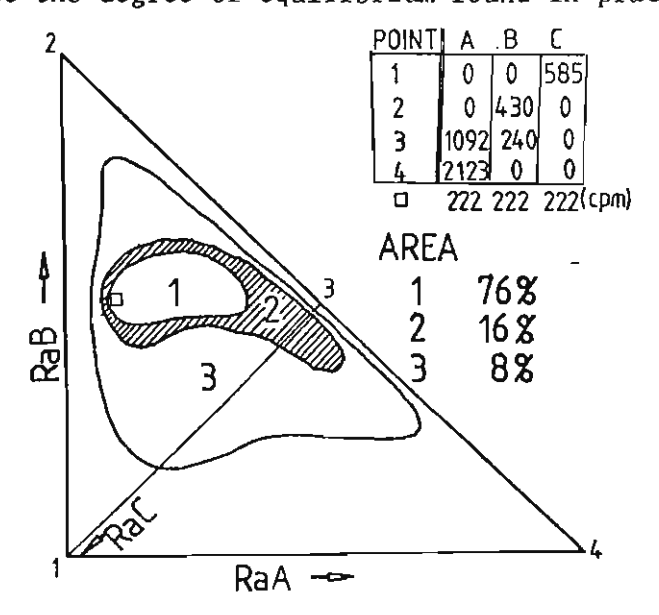


For a log-normally distributed aerosol, the average recoil escape probability illustrated above correlated well with experiment (MERCER 1976), for a 0.2µm low density particle. JONASSEN (1976) has derived correction factors for integrated filter counts for various degrees of disequilibrium of RaB.



RaB RECOIL CORRECTION FACTORS

The figure above illustrates the recoil correction for RaB for various degrees of disequilibrium with RaA for a 0.8µ AA membrane filter, assuming all recoils during sampling are redeposited and all recoils during sampling escape. This over estimates the correction since many recoil losses during counting will redeposit (range 0.15mm in air) or plate out on the detector, especially with a close geometry. DURKIN (1979) reports a survey of 271 measurements in a large number of U.S. mines. The data is normalised to 1 W.L. to illustrate the degree of equilibrium found in practice.



The square box \square represents radioactive equilibrium of the daughters, and shows gross deviations from this are unlikely. The ratio RaB: RaA should not be too small and no correction for RaB recoil losses due to a much larger RaA count necessary.

RaC

When RaB decays, the lighter β particle produces less recoil, with a maximum of 2.7eV in RaC. The effect of tunnelling through or out of the particle would be negligible. MERCER (1976) postulates that electrostatic forces would tend to retrieve most escaping RaC nuclei, so only the recoil effects of RaB need be considered.

ELECTRON MICROSCOPY

Examination of a filter specimen (Millipore AA 0.8μ) by electron microscopy was performed.

A central portion of the filter a lcm + .3mm was excised and attached to a carrier by double sided tape. A thin gold coating was applied for electron microscopy. The surface morphology was examined. Not surprisingly, no surface particles for attachment of the radon daughters were seen.

In appearance, the filter appeared very like a staghorn-type coral, with slightly large gaps between the irregular spicules serving as pores. The spicule lengths were about half the size of the largest pores.

A second sample exposed to air on the north side of the Physics Building (15 min at 201/min pumping) produced a visible discolouration of the filter.

These showed some large particles (3-10 μ) at 3000 x magnification, and a few pollen grains. Several stereoscopic views were recorded by tilting the specimen 8°. (An alternative method of producing stereoscopic views would be to move the specimen slightly laterally.) Close stereoscopic examination of the pair of photographs most likely to reveal information on the capture of particulate matter did not reveal any of the expected sub micron dust at the surface or more deeply attached. An apparent physical depth (exaggerated by the method of obtaining stereopsis) for particles 0.5μ would be about 1μ , which would not affect the alpha particle range. PALTRIDGE (1967) postulates surface charge separation as a major mechanism for removal of small charged ions (like that of the radon daughters) but points out the neutralising effect of humidity.

FILM 150 NEG 2967 MAG NEG PRINT

3000 8100

STERED PAIR OF 3967

Tim +80

IS MINS DUST PARTICLES

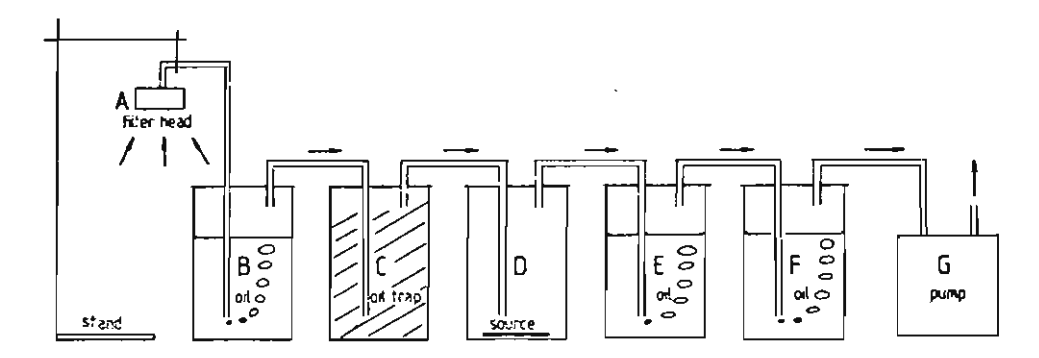
OIL EXPERIMENT

This section is not directly related to the measurement of radon daughters, but was a preliminary experiment towards using α liquid scintillation techniques.

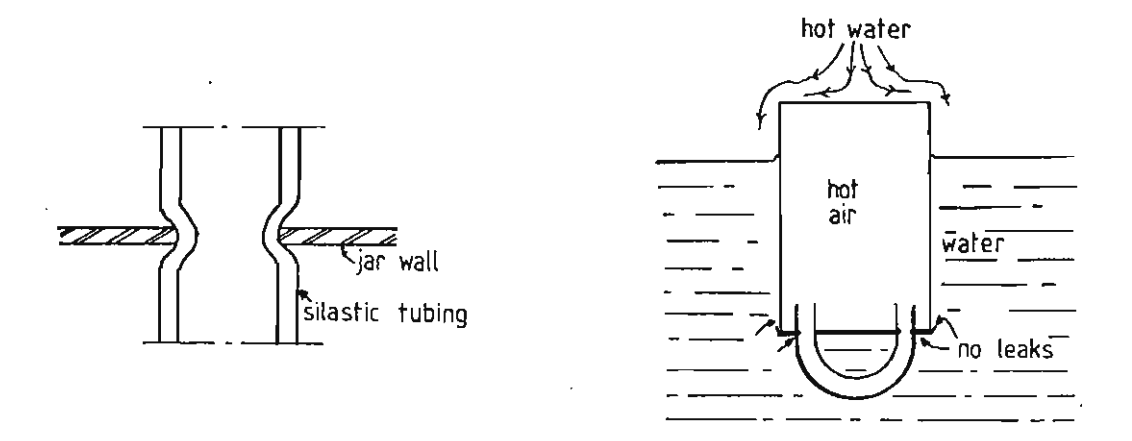
HOLADAY (1957) states "one gram of olive oil will retain in solution 125 times as much radon as compared with water".

If air containing radon is bubbled through an organic liquid (see Appendix 3) then the radon collected this way could be measured *directly* using liquid scintillation.

An experiment using domestic cooking oil was devised to find its collection efficiency for radon. A 0.2MBq (6 μ Ci) radium source was used as a radon source. The figure below shows the set up.

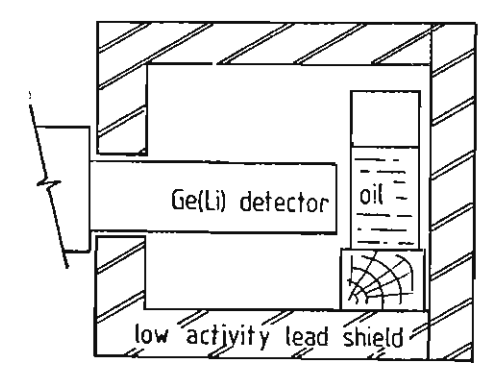


The gas tightness of the seals between the tubing and jars (below left) was tested using hot water (below).



The pump $(0.28\ 1/\text{min})$ was an aquarium pump modified to suck air. The inlet air was filtered (MILLIPORE 0.8μ pore, membrane filter) to ensure no extraneous activity entered the system. The first jar B served as a background reference.

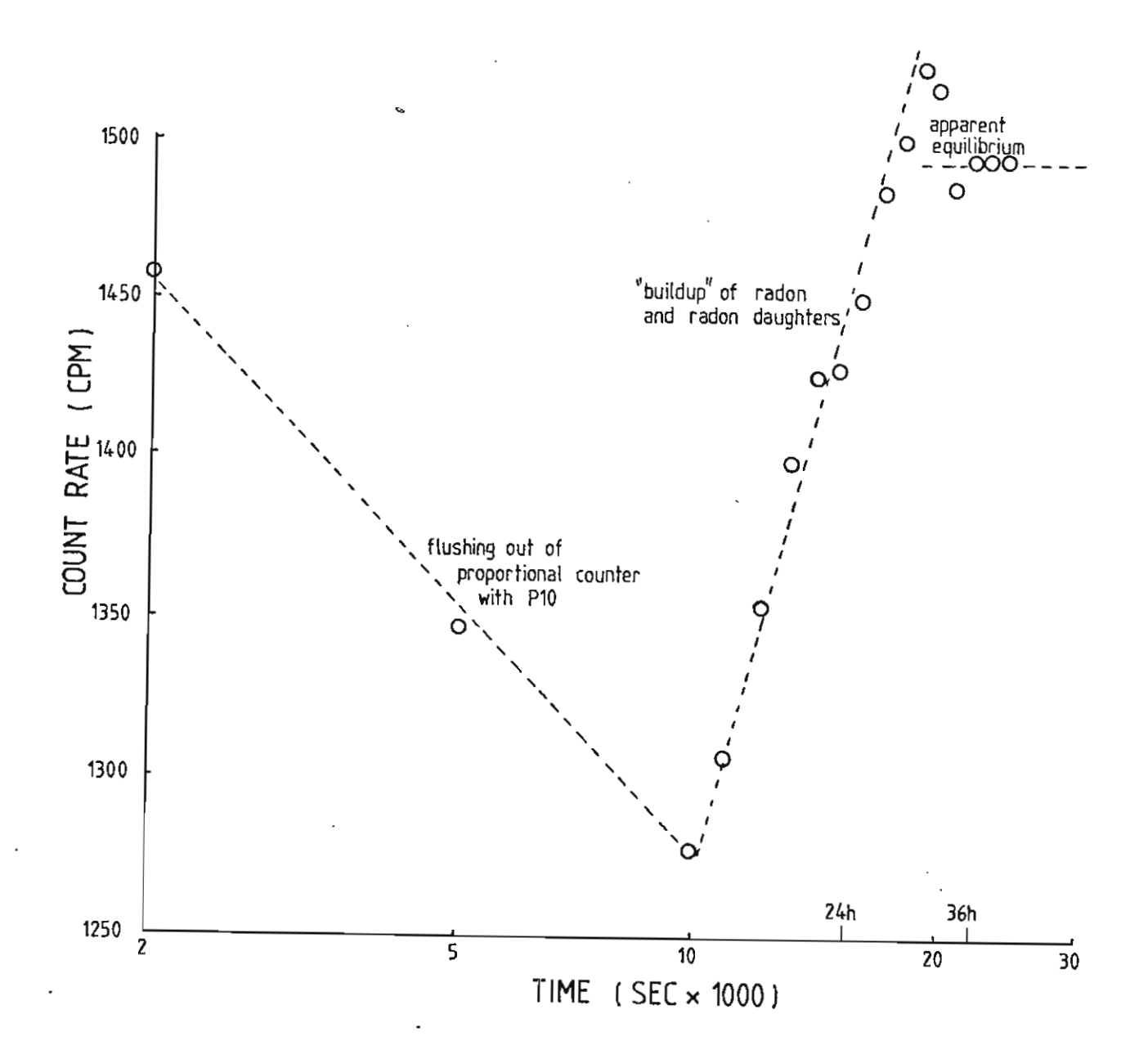
The system was run for a week and the activity in each jar measured by γ spectroscopy using a Ge(Li) detector.



The efficiency of detection, from the ratio of daughter activities in $\frac{E}{B}$ as to $\frac{F}{B}$ was 90%. The technique has possibilities, perhaps using scintillation grade tolvere as the collecting fluid, but there could be problems with evaporation.

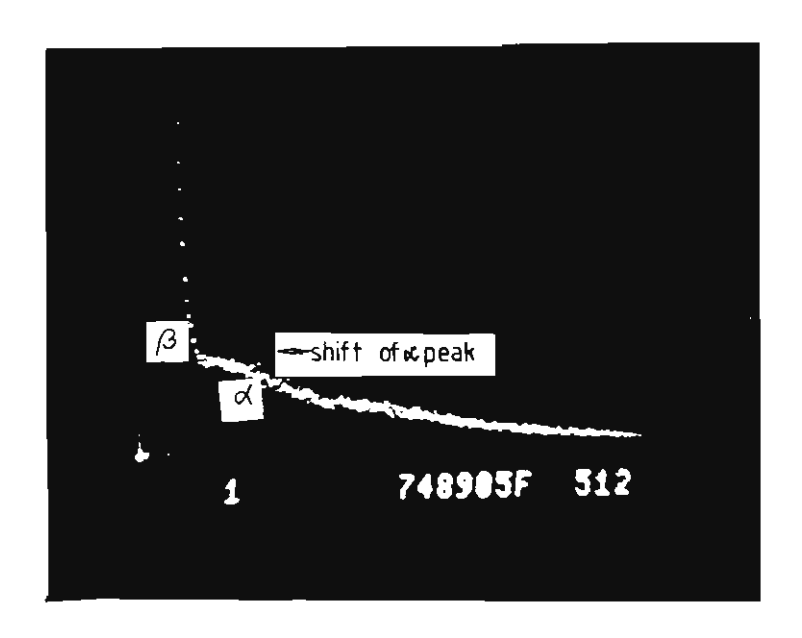
FURTHER EXPERIMENTS WITH GAS FLOW PROPORTIONAL COUNTER

Since the gas flow counter gave good α - β resolution and time resolution smaller than the half life of RaC', some work was done to try and overcome the main problem associated with the counter - its extended flushing time. The graph below shows the change in count rate with flushing.

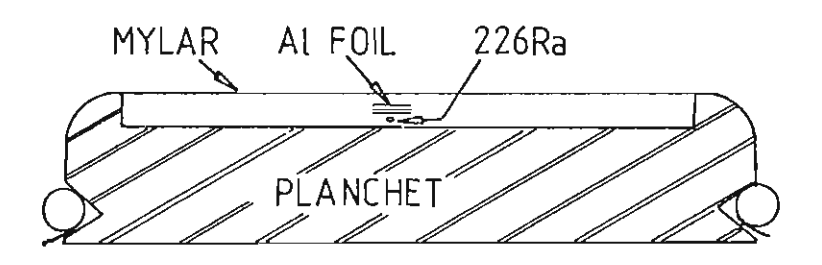


The above graph illustrates the prolonged flushing time required. The source used was a speck of radium just covered by a layer of domestic aluminium foil and glued to a small filter. The filter and foil were placed in a special planchet (see Appendix 4) designed to fit in the turret of the gas flow proportional counter. The aluminium foil was to reduce the radium background. To contain the expected release of radon, the planchet was covered with a thin $(6.35\mu,\,0.6\text{mg/cm}^2)$ polyester film (DUPONT MYLAR) to prevent escape of radon and provide a good window for α particles. This would also prevent the contamination of the detector by recoil nuclei (Appendix 6)

An effect of this approach rather than an open planchet was to shift the alpha peak towards the β peak. Further layers of aluminium foil completely eliminated any alpha peak. Apparently radon is absorbed onto solid radium surfaces (COCKETT, 1975) so the aluminium would degrade the alpha spectrum initially, and in



the later experiment, totally stop it, since it would be restrained beneath the aluminium umbrella.



PLANCHET WITH 226 Ra SOURCE COVERED BY ALUMINIUM FOIL

Further experiments were not resumed when a better radon source was developed.

MULTISCALING T1 ERROR

The data was grouped into $100\mu s$ blocks to make a smaller data block. This only produced six points, but was felt adequate to accurately describe the data.

x : time (µs)	y : counts	(background	corrected
100	761		
200	517		
300	367		
400	290		
500	149		
600	49		

A linear regression of ln y on x was performed using the HP41-C "stat pac". For a relation $y = ae^{-\lambda X}$, a value 0.004121 μs^{-1} was deduced. This corresponds to

$$T_{1_2} = \frac{\ell_{n2}}{\lambda} = 168.19 \mu s$$

An error analysis was performed (SPIEGEL, 1975 p289) using the following statistic

standard error (S.E.) =
$$\frac{t}{\sqrt{n-2}}$$
 $\frac{Syx}{Sx}$

where t = 0.741 for 4 degrees of freedom at the 50% confidence limit

$$n - 2 = 4$$

 $S_{yx}^{2} = [\Sigma(\ell_{n} y - \ell_{n} y_{est})^{2}]/n$
 $S_{x}^{2} = \overline{x^{2}} - (\overline{x})^{2}$

Evaluated, this gave

S.E. =
$$0.000277 \mu s^{-1}$$

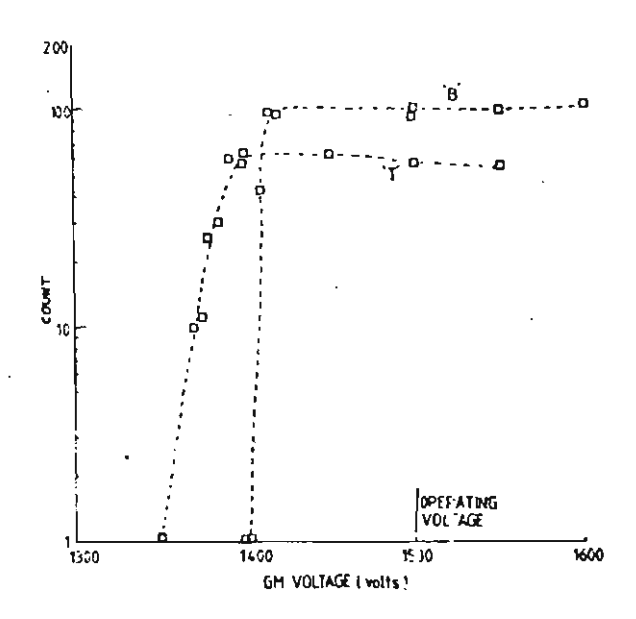
$$T_{\frac{1}{2}} = 168 \pm 168.187 \frac{0.000277}{0.004121}$$

$$= 168 \pm 9 \mu s$$

GEIGER MÜLLER TUBES

The operating characteristics of the two GM tubes (GEC model EHM2S) and scalers were checked to see whether the settings used fell on the "Geiger plateau". The figure below shows the operating voltage of 1500V is correct.

GM TUBE OPERATING CHARACTERISTICS



The letters T and B refer to the top and bottom GM/scaler combination. The characteristics of T are poorer than that of B partly due to source/detector geometry and partly due to age of the GM tube.

A factor which was not measured was the *effective area* of the window and the position of the sensitive volume of the GM tube behind the window. The best approach would have been an empirical determination of the effect of these factors using the sources.

DEAD TIME

Consider the dead time correction to a count n to be given by n.

 $m_i = \frac{n_i}{1 - n_i \tau}$ where τ is the dead time.

Then for a split source producing three counts n_1 , n_2 and n_{12} .

$$m_1 + m_2 = m_{12}$$

i.e.
$$\frac{n_1}{1-n_1\tau} + \frac{n_2}{1-n_2\tau} = \frac{n_{12}}{1-n_{12}\tau}$$

Multiply through by the denominator and rearrange.

$$n(1-n_{2}\tau)(1-n_{12}\tau) + n_{2}(1-n_{1}\tau)(1-n_{12}\tau) - n_{12}(1-n_{1}\tau)(1-n_{2}\tau) = 0$$
i.e.
$$\tau^{2}(n_{1}n_{2}n_{12} + n_{1}n_{2}n_{12} - n_{1}n_{2}n_{12})$$

$$-\tau(n_{1}n_{2} + n_{2}n_{12} + n_{1}n_{2} + n_{2}n_{12} - n_{2}n_{12})$$

$$+ n_{1} + n_{2} - n_{12} = 0$$

$$\tau^{2}(n_{1}n_{2}n_{12} - 2n_{1}n_{2}\tau + (n_{1} + n_{2} - n_{12}) = 0$$

This is of the form $a^2 + b + c = 0$ and

has roots
$$\tau = \frac{-b \pm \sqrt{b^2 - 4ac}}{2a}$$

$$\tau = \frac{2n_1n_2 \pm \sqrt{4}n_1^2 + n_2^2 - 4n_1n_2n_3(n_1 + n_2 - n_{12})}{2n_1n_2n_1}$$

$$= \frac{1}{n_{12}} \left[1 \pm \left(1 - \frac{(n_1 + n_2 - n_{12})n_{12}}{n_1n_2} \right)^{\frac{1}{2}} \right]$$

The error in this measurement is soluble using the chain rule (BRAGG, 1974 p95) and maximising the error. (The relation $\partial n_i = \lceil \overline{n_i} \rceil$ is used.) The error in τ is then

$$\delta \tau = \left| \frac{\partial \tau}{\partial n_{12}} \delta n_{12} \right| + \left| \frac{\partial \tau}{\partial n_{1}} \delta n_{1} \right| + \left| \frac{\partial \tau}{\partial n_{2}} \delta n_{2} \right|$$

Separating the differentials for ease of handling gives

$$\frac{\delta \tau}{\partial n_{12}} = -\frac{1}{n_{12}^2} \left[1 - \left(1 - \frac{n_{12}(n_1 + n_2 - n_{12})^{\frac{1}{2}}}{n_1 n_2} \right) \right]$$

$$+ \frac{1}{n_{12}} \left[\frac{1}{2} \left\{ 1 - \frac{n_{12}(n_1 + n_2 - n_{12})}{n_1 n_2} \right\}^{\frac{1}{2}} \times \frac{n_{12}}{n_2} \right]$$

$$\frac{\partial \tau}{\partial n_1} = \frac{1}{n_{12}} \left[\frac{1}{2} \left\{ 1 - \frac{n_{12}(n_1 + n_2 - n_{12})}{n_1 n_2} \right\}^{\frac{1}{2}} \times \frac{n_{12}}{n_2} \right]$$

$$\frac{\partial \tau}{\partial n_2} = -\frac{1}{N_{12}} \left[\frac{1}{2} \left\{ 1 - \frac{n_{12}(n_1 + n_2 - n_{12})}{n_1 n_2} \right\}^{\frac{1}{2}} \times \frac{n_{12}}{n_1} \right]$$

The relations (i)
$$\frac{\partial}{\partial x} \sqrt{u} = \frac{1}{2\sqrt{u}} \cdot \frac{\partial u}{\partial x}$$

$$(ii)$$
 (gh) = g h + gh are used.

This may be written as

$$\delta \tau = \frac{\sqrt{n_{12}}}{n_{12}^2} \left\{ a \left[\frac{n_1 n_2 + n_1 + n_2 - 1}{n_1 n_2} - 1 \right] + \frac{n_1}{2an_2} + \frac{n_2}{2an_1} \right\}$$

where a
$$= \left[1 - \frac{n_{12}(n_1 + n_2 - n_{12})}{n_1 n_2}\right]^{\frac{1}{2}}$$

This is a pessimistic approach and gives the worst case, assuming the components are related. If it is assumed the components are independent,

then
$$\delta \tau = [| \sim |^2 + | \sim |^2 + | \sim |^2]^{\frac{1}{2}}$$

Graphically this is just

or

linear addition or

~diagonal of cube.

The analysis is a simplified case and assumes the background contribution is very small and can be ignored. The background should still be subtracted from each count. A program was written for a small programmable calculator (HP41C) to calculate the dead time and associated error.